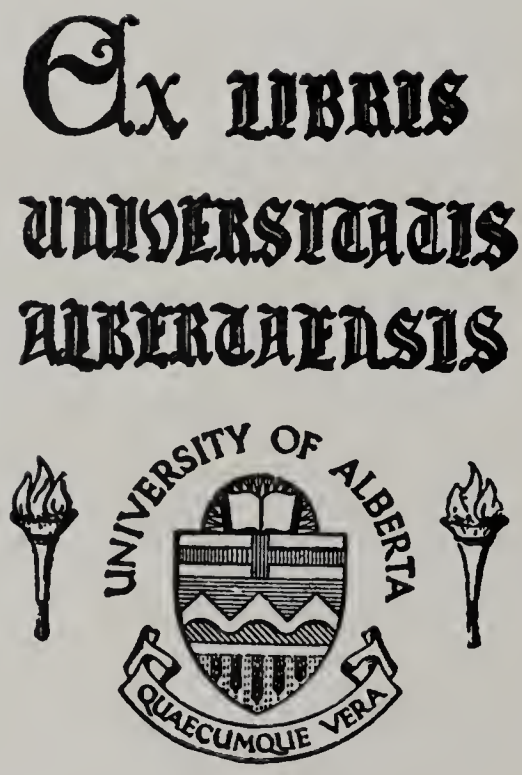

University of Alberta
Printing Department

THE UNIVERSITY OF ALBERTA

"GAS HYDRATES IN THE PROPANE-CARBON DIOXIDE SYSTEM"

BY

B.R. MEHTA

A THESIS

SUBMITTED TO THE FACULTY OF GRADUATE STUDIES

IN PARTIAL FULFILLMENT OF

THE REQUIREMENTS FOR THE DEGREE OF

MASTER OF SCIENCE IN CHEMICAL ENGINEERING

FACULTY OF ENGINEERING

DEPARTMENT OF CHEMICAL AND PETROLEUM ENGINEERING

EDMONTON, ALBERTA

JUNE, 1965

THE UNIVERSITY OF ALBERTA

FACULTY OF GRADUATE STUDIES

The undersigned certify that they have read, and recommend to the Faculty of Graduate Studies for acceptance, a thesis entitled "Gas Hydrates in the Propane-Carbon Dioxide System" submitted by B.R. Mehta in partial fulfillment of the requirements for the degree of Master of Science in Chemical Engineering.

ABSTRACT

The propane-water system was studied in three phase (hydrate - water rich liquid - gas) equilibrium in the region of 32°F to 42.3°F and 25 psia to 80 psia. This equilibrium was terminated at the four phase point due to the appearance of the propane rich liquid phase at T = 42.3°F and P = 80 psia.

The carbon dioxide - water system was investigated in the same three phase equilibrium in the region of 32°F to 50.3°F and 172 psia to 648 psia. The quadruple point was observed at T = 50.3°F and P = 648 psia.

The ternary system CO_2-C_3H_8-H_2O was studied in the three phase equilibrium region at various compositions. The four phase locus was determined and a maximum temperature point was observed in this locus at 56.7 °F.

The potential parameters for CO_2 and C_3H_8 molecules were computed by fitting the experimental dissociation pressure at 0°C. They were σ = 3.96 Å and ε/k = 148 °K for the carbon dioxide molecule, while σ = 4.80 Å and ε/k = 278 °K for the propane molecule. Using these parameters, Langmuir constants were calculated as a function of temperature. These constants were used to predict initial hydrate formation conditions for CO_2-H_2O and C_3H_8-H_2O systems. The average deviations between the predicted and experimental results were 6% and 4% for the CO_2-H_2O and C_3H_8-H_2O systems respectively.

ACKNOWLEDGEMENTS

An expression of sincere gratitude is offered to Dr. D. B. Robinson for his invaluable guidance and encouragement throughout the course of this project.

Acknowledgements are made to Mr. K. Balcombe and Mr. G. Walsh and his staff for their help and cooperation in constructing the equipment. Thanks are also expressed to Miss W. Silcox for the typing of the thesis. The author wishes to express his thanks to all those friends and colleagues who contributed their time and efforts in offering helpful suggestions and by proofreading the manuscript.

Financial assistance by the National Research Council of Canada is gratefully acknowledged.

TABLE OF CONTENTS

LIST OF TABLES

LIST OF FIGURES

INTRODUCTION

A gas hydrate is an inclusion compound in which two or more components are associated without ordinary chemical union, but through a complete enclosure of one set of molecules in a suitable structure formed by another. Such compounds were classified as Clathrates by Powell[35]. They are characterized by a cage-like structure which is formed by water molecules. The hydrate forming molecules are enclosed in these cavities.

The process of hydrate formation can be represented as,

$$R_{(g)} + n\ H_2O_{(l)} \rightleftharpoons R \cdot n\ H_2O_{(s)}$$

where a hydrate forming gas R combines with n molecules of water to form a hydrate $R \cdot n\ H_2O$. As the forces stabilizing the hydrate are purely physical in nature, a gas hydrate is not a stoichiometric compound. The experimental value of n varies from 5.70 to 17.0 depending upon the hydrate forming molecule and the structure of hydrates formed.

The type of molecules which may be bound in the cavities is very diverse, as it includes O_2, N_2, CH_4, C_2H_2, CH_3CF_2Cl etc. and even the noble gases A, Kr, Xe. Once such a molecular complex is formed, it may persist under conditions where it is no longer thermodynamically stable. An example is the complex with Argon which can be kept indefinitely in an ordinary bottle, although the equilibrium pressure of argon over the crystal amounts to several atmospheres at room temperature.

Faraday, in 1810, discovered the first gas hydrate of chlorine. Villard[53] and de Forcrand[11, 12, 13] studied the hydrate forming conditions and hydrate formulas of hydrocarbon and non-hydrocarbon compounds. Hammerschmidt's[15] publications confirmed that gas hydrates were responsible for the plugging of natural gas transmission lines. His work provided an impetus to research in the area of process development to inhibit hydrate formation. Methods and means were proposed for the partial dehumidification of the natural gas. This technique was successfully used to prevent condensation of water vapors in the transmission lines, at operating pressures and temperatures which were also favourable for hydrate formation. Various dehydrating agents[4, 16] were proposed, one of which, diethylene glycol, is now being used extensively.

To be able to predict the initial hydrate formation conditions of a gas mixture of known composition, the concept of vapor-solid equilibrium was proposed by Wilcox et al[60]. This method proved useful for engineering calculations[25], although it could not account for the effect of composition on the vapor-solid equilibrium constants of multi-component systems.

Claussen[6] and von Stackelberg[50, 51] studied the crystal structures of gas hydrates through the use of the x-ray diffraction technique. All hydrates, according to these studies, crystallize in either of two structures, Structure I or Structure II. Dimensions and other details of these structures are given

in Appendix B. Although it is difficult with this information to predict exactly which molecules will form gas hydrates, the dimensions of the cavities may restrict the number of gases which can form hydrates. Any gas whose molecular size is greater than 6.7 Å cannot form hydrates. Theoretically there may not be any restriction on the smaller molecules. However, it is found that smaller molecules like hydrogen and helium are not retained within the frame. Gases like ammonia and halogens which show specific chemical reaction with water molecules do not form gas hydrates.

Dimensional limitations and geometrical shape of the cavities in Clathrate compounds suggested uses in purification and separation processes[3, 36]. Schaeffer[44] has reviewed extensively the applications of clathration as a unit process in the petroleum refining and petro-chemical industries. Parent[34] has evaluated the proposal for storage of natural gas as hydrates. Very recently, gas hydrates are gaining importance as potential means for desalination of sea-water[2]. Propane was studied[27] on a pilot-plant scale and preliminary process design calculations[45] were made to compare the feasibility of this process with other processes available for demineralization of sea-water.

In order to study the effect of one gas on the hydrate formation conditions of the other gas, ternary systems A-B-H_2O were investigated by Deaton and Frost[8, 9, 10], Reamer et al[40], Otto[32] and Jhaveri[20]. As carbon dioxide and propane are

constituents of the natural gas, it was decided to study the initial hydrate formation conditions of the systems CO_2-H_2O, C_3H_8-H_2O and CO_2-C_3H_8-H_2O. The three phase HL_1G equilibrium of the binary system, propane-water, has been investigated by Miller and Strong[42] and of the binary system CO_2-H_2O has been studied by Unruh and Katz[52].

The initial hydrate formation conditions of certain ternary systems containing either CO_2 or C_3H_8 have been reported in the literature for CH_4-C_3H_8-H_2O[10], CH_4-CO_2-H_2O[52] and C_3H_8-C_3H_6-H_2O[40]. The temperatures of the hydrate formation are lower than the critical temperature of CO_2 and C_3H_8 in the ternary system CO_2-C_3H_8-H_2O. In other words, the hydrate forming gases will appear in the non-aqueous liquid phase L_2 at certain pressures. Such a system would, therefore, exhibit a univariant four phase (HL_1L_2G) equilibrium.

Platteeuw and van der Waals[54, 55, 56] and Barrer and Stuart[3] proposed a statistical thermodynamic approach to predict the phase behaviour of gas hydrates in three phase equilibria, HIG and HL_1G. This solid solution theory has been used for pressure-composition calculations of the ternary systems C_3H_8-H_2S-H_2O and C_3H_8-CH_4-H_2O in the three phase HIG equilibrium. It was decided in this work to extend this theory to the study of initial hydrate forming conditions of the system CO_2-C_3H_8-H_2O in three phase equilibrium HL_1G.

THEORETICAL PROGRAM

A. Phase Behaviour of Gas Hydrates

The total number of phases present at the equilibrium pressure and temperature in any system is given by Gibb's Phase-rule which states that,

$$F + P = C + 2$$

where,

F = number of degrees of freedom

P = number of phases present

C = number of components

From this relationship, it may be deduced[42] that the addition of a component to a system adds a degree of freedom to all features represented by the system. In other words, areas will generate volumes, lines will generate surfaces and points will generate lines. These features will have one extra degree of freedom, but they will not be changed in designation. That is, a point representing vapor-solid-liquid equilibrium for a one component system will generate a line in space on the addition of a second component, but this line will represent the equilibrium between the same phases, namely vapor-solid-liquid.

Termination of a particular type of phase equilibrium may be brought about by the addition of a phase, by the loss of a component, or by attainment of critical conditions. The appearance of a new phase decreases the degree of freedom by one. In light of these general rules, Otto[32] and Parent[34] have

described the essential features of the phase diagrams of binary and ternary systems.

The phase behaviour of ternary systems such as A-B-H_2O can be classified into two types:

(i) Systems in which hydrates of A-B-H_2O grow in one structure.

Systems of this type are illustrated in Figure 1. They exhibit complete miscibility of the solid solutions, that is, hydrates of A-H_2O and B-H_2O are formed in either of the structures. The ternary system CH_4-H_2S-H_2O is an example of this type of phase behaviour. This particular ternary mixture, as studied by Noaker and Katz[31], showed a continuous range of mixed hydrates of Structure I. In this system, since the temperatures of hydrate formation were higher than the critical temperature of CH_4, a methane-rich liquid phase did not appear at any pressure. On the other hand, in a system like CO_2-H_2S-H_2O both of the hydrate forming components will appear in the non-aqueous liquid phase, L_2. As shown in Figure 1, hydrates in the binary systems CO_2-H_2O and H_2S-H_2O grow in Structure I. Lines joining two pairs of quadruple points, one at the freezing point ($H_I IL_1 G$) and the other above the freezing point of water ($H_I GL_1 L_2$), describe the univariant four phase equilibria. Due to lack of experimental data, the exact shape of these four-phase locii is not known.

An example of complete miscibility in Structure II hydrates is the ternary system propane-propylene-water. This system has been studied by Reamer[40].

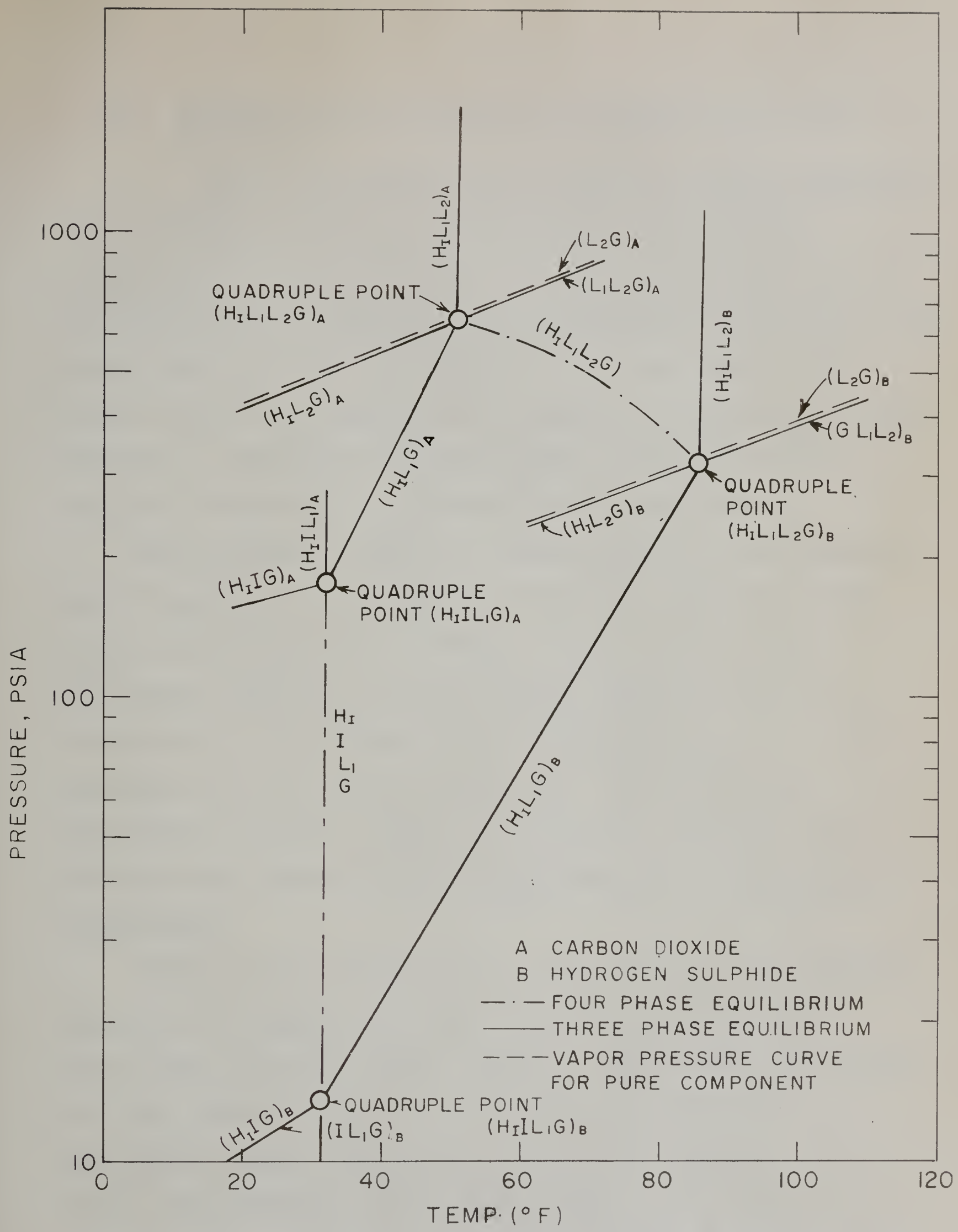

FIG. 1 P-T PROJECTION OF PHASE BEHAVIOUR OF THE SYSTEM $H_2S-CO_2-H_2O$ IN WHICH THE BINARY SYSTEM H_2S-H_2O AND CO_2-H_2O FORM STRUCTURE-I HYDRATES.

(ii) Systems in which hydrates of A-B-H_2O grow in both structures.

These are illustrated in Figure 2, and are generally known as double hydrates, characterized by the partial miscibility of solid solutions. In other words, hydrates of the binary system A-H_2O may grow in Structure I and those of the system B-H_2O may grow in Structure II or vice versa. The ternary system CO_2-C_3H_8-H_2O is an example of this type of phase behaviour. The binary systems CO_2-H_2O and C_3H_8-H_2O form hydrates of Structure I and Structure II respectively.

When propane is added to carbon dioxide at the quadruple point $(H_IL_1IG)_A$, the pressure will increase until the mixed hydrate of Structure II is formed. Thus the four phase equilibrium $(H_IIL_1G)_{A,B}$ for the three component system is terminated at the quintuple point $(H_IH_IIL_1L_2G)_{A,B}$ due to the appearance of a new hydrate phase H_{II}. The three-phase equilibrium branches, $(H_IIG)_A$ and $(H_IL_1G)_A$, therefore lie below the four phase branches $(H_IH_IIIG)_{A,B}$ and $(H_IH_IIL_1G)_{A,B}$ respectively.

Owing to the presence of a solid phase H_I, the branches $(H_IL_2G)_A$ and $(L_1L_2G)_A$ are shown below the vapor pressure curve $(L_2G)_A$ for pure carbon dioxide. Since water and propane are less volatile than carbon dioxide, the four phase equilibrium branch $(H_IH_IIL_2G)_{A,B}$ lies below $(H_IL_2G)_A$. As a result, the quintuple point $(H_IH_IIL_1L_2G)_{A,B}$ is located at a lower pressure and lower temperature than the quadruple point

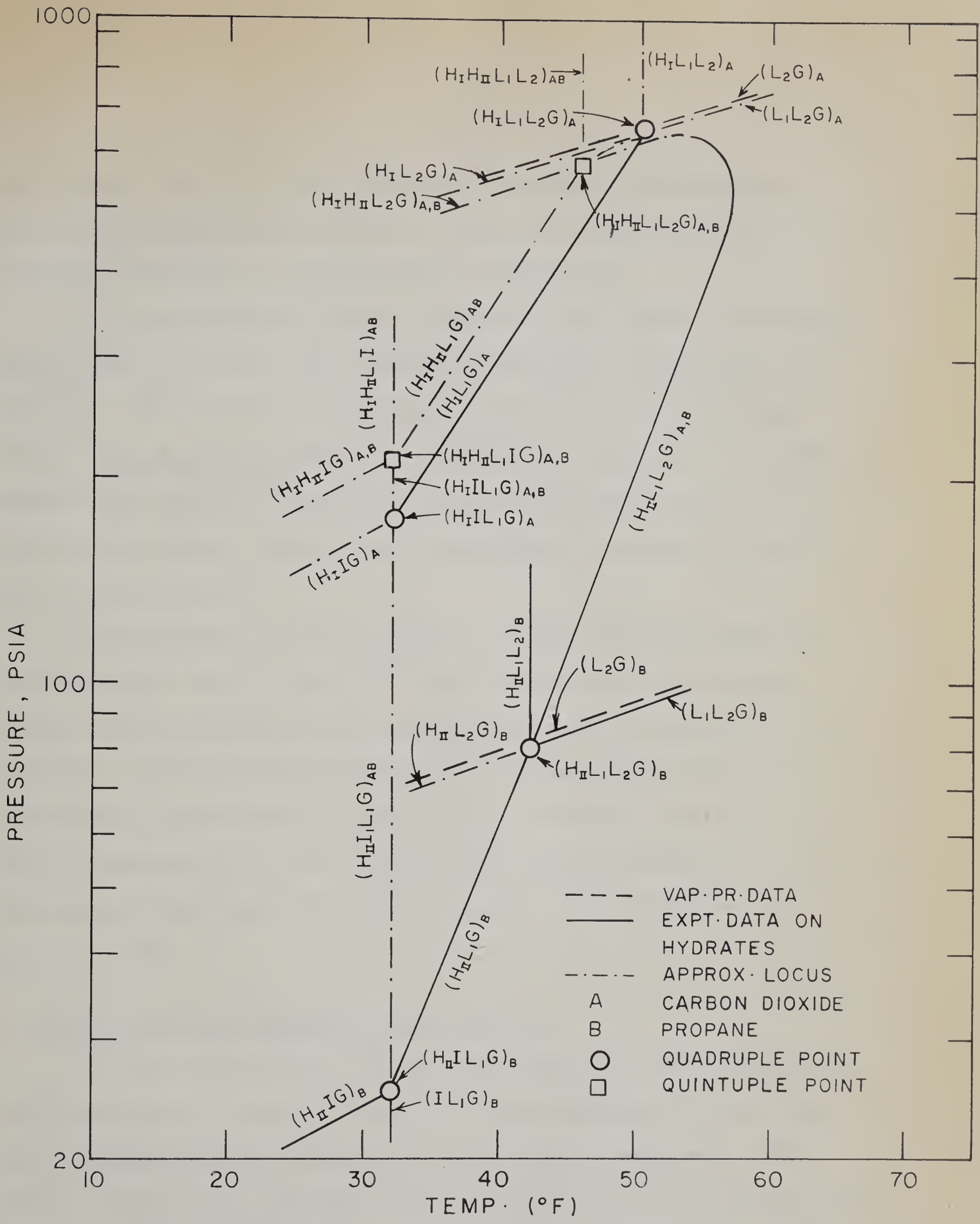

FIG·2 PHASE BEHAVIOUR OF THE TERNARY SYSTEM $CO_2-C_3H_8-H_2O$ IN WHICH THE SYSTEM CO_2-H_2O FORM STRUCTURE I AND THE SYSTEM $C_3H_8-H_2O$ FORM STRUCTURE II HYDRATES

$(H_I L_1 L_2 G)_A$. As it is not possible to detect the presence of H_I and H_{II} phases individually, there is no experimental evidence available to support these deductions.

It is interesting to note that the four phase equilibrium $(H_{II} L_1 L_2 G)_{A,B}$ starts from the quadruple point $(H_{II} L_1 L_2 G)_B$ of propane. This locus can be terminated only at the quintuple point $(H_I H_{II} L_1 L_2 G)_{A,B}$ where a new phase H_I appears. A maximum temperature point is observed on the four phase $(H_{II} L_1 L_2 G)_{A,B}$ equilibrium curve. Beyond this temperature, hydrates do not form in Structure II.

Co-existence of the H_I and H_{II} phases was confirmed by Platteeuw and van der Waals[56] when they studied pressure-composition diagrams of the CH_4-C_3H_8-H_2O and H_2S-C_3H_8-H_2O systems. An interesting exception to these discussions is provided by the system H_2S-CH_3CHF_2-H_2O in which the two binary systems H_2S-H_2O and CH_3CHF_2-H_2O form hydrates of Structure I only, but the ternary system forms hydrates of Structure II.

B. Solid Solution Theory of Gas Hydrates

A common feature of all gas hydrates is a host lattice of water molecules, which by itself is thermodynamically unstable, but is stabilized by inclusion of the second component. The forces binding this component may be similar to the intermolecular forces in liquids[54]. It seems natural therefore, to regard them as a solid solution of the second component in the host lattice.

Platteeuw and van der Waals[56] derived, through the use of statistical thermodynamics, a set of equations which describe the phase behaviour of Clathrates. The basic equations are,

$$\mu_Q = \mu_Q^\beta + RT \sum_i \nu_i \ln \left(1 - \sum_k y_{ki}\right) \qquad (1)$$

$$y_{ki} = \frac{C_{ki}\, p_k}{1 + \sum_J C_{Ji}\, p_J} \qquad (2)$$

$$C_{ki} = \frac{1}{k\,T} \cdot \frac{h_{ki}\,(T,V)}{\phi_k\,(T)} = \frac{h_{ki}\,(T,V) \cdot \lambda_k}{p_k} \qquad (3)$$

Equation (1) is a generalized form of Raoult's law when solute-solvent intereaction is neglected. The total chemical potential μ_Q is made of contributions due to the empty lattice, represented by μ_Q^β and that due to encaged molecules, represented by the summation term in equation (1).

Equation (2) is equivalent to Langmuir's isotherm for localized adsorption without interaction between the adsorbed molecules. The probability of finding a molecule k in cavity of i type is given by y_{ki}. The equilibrium pressure or dissociation pressure p_k can be replaced by a corresponding fugacity term if the system behaves non-ideally.

Equation (3) defines the Langmuir constant C_{ki} which is a function of temperature only for a given molecule. The

calculations of Langmuir constants are illustrated in Appendix C.

In order to calculate the partition function h_{ki} (T,V), Platteeuw and van der Waals[56] applied the Lennard-Jones-Devonshire's cell theory which is appropriate in this case because the gas molecule is moving in an almost spherical cage made up of water molecules. They calculated the force field by using L-J-D 12/6 potential model. The agreement between calculated and observed values of the dissociation pressure is quite good for the monoatomic gases like A, Kr, etc. and to a lesser extent for the quasi-spherical molecules like CH_4, SF_6. However, the agreement becomes very unsatisfactory in the case of non-spherical molecules like CO_2, C_2H_6 and N_2.

This poor agreement may be due to

(i) hindered rotation of the rod-like molecules in their cavities,

(ii) failure of the central force field approximation to describe the interaction between a solute molecule and a molecule in the host lattice,

(iii) the chemical potential of the lattice may not be independent of the solute occupation,

(iv) the shape and size of encaged molecules cannot be neglected when evaluating overall cavity potential.

The third and fourth reasons were investigated by McKoy[29]. To a good degree of approximation, it was confirmed by McKoy,

that the chemical potential of the lattice is independent of the solute occupation of the cavity. This shows that the possible lattice distortions appear to have a very small effect on the thermodynamic properties of the lattice. Improved dissociation pressures were obtained[29] by accounting for the effect of the shape and size of the molecule.

To obtain the coefficients for the Virial equation of state, various potential functions are used. These potential functions are based on a particular model proposed for the gas molecule. Realistic potential functions must be used to fit the experimental data over large temperature ranges. In addition, more realistic potential functions were proposed to obtain force constants, (ε/k) and (σ). These constants could be used to predict the behaviour of the gas.

The Lennard-Jones (6-12) potential has been widely used for the calculation of the properties of the matter in the gaseous, liquid and solid states. This potential function is defined in terms of the force constants. These constants may be determined by analysis of the second virial coefficient data. McKoy[29] found that the dissociation pressures of gas hydrates were more sensitive to the parameters of the intermolecular potentials than were second virial coefficient data. The values of these parameters, (ε/k) and (σ), found in the literature were very different even for the rare gases which have been most studied.

For equilibrium between hydrate and the stable crystalline α-form (ice) of lattice, we have,

$$\mu_Q = \mu_Q^{\alpha} \tag{4}$$

Let $$\Delta \mu\ (T,P) = \mu_Q^{\beta} - \mu_Q^{\alpha} \tag{5}$$

Since the α and β forms represent the pure crystalline states of the lattice former, the difference in chemical potential ($\Delta \mu$) is a function of pressure and temperature alone.

Substituting equation (1) and (4) into equation (5), we obtain,

$$-\frac{\Delta\mu}{RT} = \sum_i \nu_i \ln\left(1 - \sum_k y_{ki}\right) \tag{6}$$

Substituting for y_{ki} in equation (6) from equation (2), we get,

$$\Delta\mu = RT \sum_i \nu_i \ln\left(1 + \sum_k c_{ki}\, p_k\right) \tag{7}$$

Equation (4) is an essential condition for three phase equilibrium, HIG, below the freezing point of water. At temperatures above the freezing point however, the stable liquid form L_1(water) exists in equilibrium with other phases. For equilibrium between water and hydrate, we have,

$$\mu_Q = \mu_Q^{L} \tag{8}$$

Let $\Delta\mu = \mu_Q^\beta - \mu_Q^L$ (9)

Since some gas is dissolved in the liquid phase L_1, the chemical potential difference in equation (9) is now a function of pressure, temperature and composition.

Assuming that the water in contact with the hydrate behaves like an ideal solution, we have,

$$\mu_Q^L = (\mu_Q^L)^* + RT \ln x_Q \quad (10)$$

where μ_Q^L is a function of pressure, temperature and composition while $(\mu_Q^L)^*$ is a function of temperature and pressure only.

Substituting equation (10) in (9),

$$\Delta\mu = \mu_Q^\beta - (\mu_Q^L)^* - RT \ln x_Q$$

Let $\Delta\mu' = \mu_Q^\beta - (\mu_Q^L)^*$

Then,

$$\Delta\mu = \Delta\mu' - RT \ln x_Q \quad (11)$$

where $\Delta\mu'$ is a function of P and T only.

Substituting equation (7) in (11), we get,

$$\Delta\mu' = RT \sum_i \nu_i \ln (1 + \sum_k C_{ki} p_k) + \ln x_Q \quad (12)$$

At constant temperature, the effect of pressure on chemical potential difference is given by,

$$(\partial\Delta\mu'/\partial P)_T = \Delta V' \quad (13)$$

Integrating equation (13) at constant T,

$$\Delta\mu' = \Delta\mu'_o + \Delta V' (P - P_o) \qquad (14)$$

Equation (14) enables one to calculate $\Delta\mu'$ values at any pressure P and for any component with respect to $\Delta\mu'_o$ and P_o values of a reference component at the same temperature. It is assumed that $\Delta V'$ is independent of pressure. The values of $\Delta V'$ for Structure I and Structure II hydrates are reported in the literature[56]. The quantities $\Delta\mu'_o$ and P_o for a reference component are computed by using equation (12). Methane and sulfur hexafluoride were chosen as the reference components for Structure I and Structure II hydrates respectively.

Using this approach, Marshall, Kobayashi and Shozaburo[26, 27, 46, 47] investigated A-N_2-H_2O and CH_4-A-H_2O systems in three phase (HL_1G) equilibrium. Their theoretical calculations together with the experimental results indicated that the solid solution theory could be satisfactorily used for the hydrates of non-spherical molecules in the three phase hydrate - water rich liquid - gas, equilibrium.

EXPERIMENTAL PROGRAM

A. Equipment

The equipment used for this work was essentially the same as that used by earlier workers, Snell[49] and Jhaveri[20] for their work on gas hydrates. The major components of this equipment are shown in the schematic diagram, Figure 3.

The equilibrium cell was made from a Penberthy liquid level gauge capable of withstanding 6000 psia at 250°F with a test pressure of 9000 psia. The cell body was made of 316 type stainless steel and had glass windows, one on each side. These glass windows, manufactured by Corning Glass Works, were rated at 9000 psia at 100°F.

The cell was, as shown in Figure 3, jacketted by a lucite shell of 3/8" thickness and 8" O.D. The top and bottom of the cell were connected to the outside of the jacket through rotary seals, one on either side. These seals rest on bearings and prevent leakage of the cell contents when the cell is rocking. Gaskets made from 1/8" thick Teflon sheet were used to seal the glass-to-metal connections. The high pressure tubings, valves and other connections were supplied by Autoclave Co. and were rated at 10,000 psia pressure. The cell could be rocked through an arc of 30-35 degrees by an eccentric driven by a 1/6 H.P. motor.

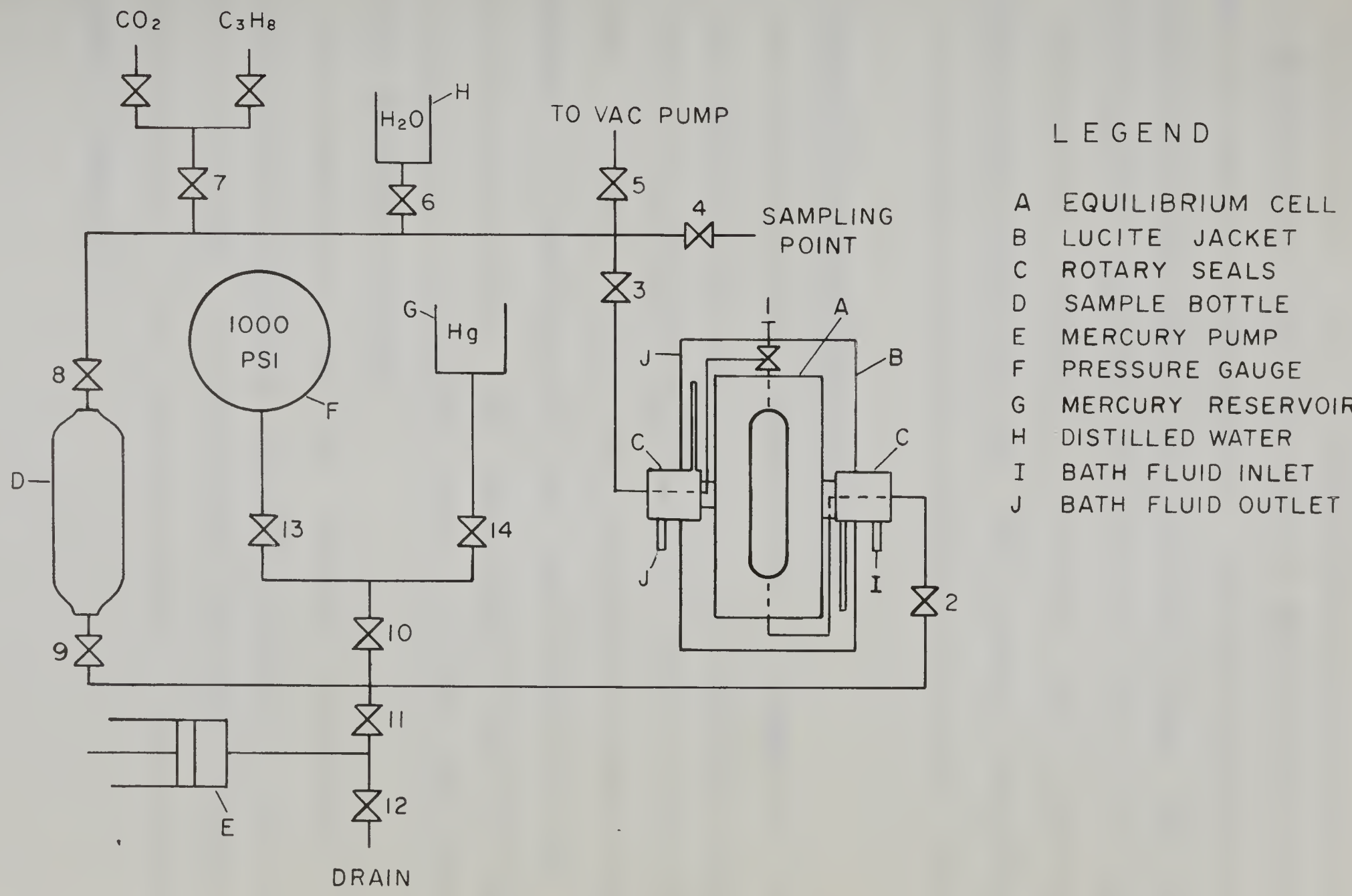

FIG·3 SCHEMATIC DIAGRAM OF THE EQUIPMENT

B. Pressure Measurement and Generation

A hand driven, positive displacement mercury pump of 265 cc displacement volume and rated at 8000 psia was used to change the pressure in the system. Chemically purified and once distilled mercury was used as the confining fluid. The volume displaced could be read from the graduated scale on the pump.

Pressure was measured by a 0-1000 psi Heise gauge having a minimum scale reading of 2 psi. The pressure calibration of this gauge was checked with a standard dead weight tester.

C. Temperature Measurement and Control

To facilitate visual observations, a transparent fluid with low freezing point was chosen for heat exchange purposes. This fluid was a petroleum based solvent having a flash point of 110°F. The cell contents were maintained at the desired temperature by circulating the bath fluid around the cell through the lucite shell. The temperature of the bath fluid was controlled by a bimetallic strip controller supplied by American Instrument Company.

The temperature of the cell contents was measured by an Iron-Constantan thermocouple, inserted through the side of the stainless steel body. A potentiometer was used to measure the voltage difference. The calibration curve for the thermocouple is shown in Appendix A.

D. Materials

The mercury used for this work was chemically purified and distilled once. The water used for the experimental work was deaerated and doubly distilled. The carbon dioxide and propane used for hydrate formation experiments were 99.8% and 99.5% pure respectively.

E. Experimental Procedures

The experimental procedures included preparation of the gas mixtures, observation of the initial hydrate formation conditions, and analysis of the gas samples.

(i) Preparation and Analysis of Gas Mixtures

A mixture of the desired composition of carbon dioxide and propane was prepared by adjusting the pressures of the gas cylinders. From the compressibility data for the individual components and their mixture[1, 21, 39], these pressures were calculated since the volume of the sample bottle and the temperature were known. These mixtures were then analyzed chromatographically. The chromatographic analysis is described in Appendix A.

The lines and sample bottle D (See Figure 3) up to valve 9 were evacuated. Propane was then bled through the system and evacuated again. Propane was taken first into the sample bottle D until the gauge on the propane cylinder indicated the desired pressure. Carbon dioxide was then added to propane

until the desired pressure of the mixture was read on the gauge. Propane was charged first because the propane cylinder was at a lower pressure than the carbon dioxide cylinder. Valves 7 and 8 were then closed. A sample of this mixture was then taken from the sampling point and analyzed on the gas chromatograph.

(ii) Initial Hydrate Formation Experiments

Above the freezing point of water, for three phase equilibrium HL_1G, of the ternary system CO_2-C_3H_8-H_2O, two degrees of freedom are available to the system. This equilibrium will, therefore, generate a surface on the P-T diagram. Such an equilibrium with a constant gas composition will generate a line on this surface. Thus for a fixed composition parameter of a ternary system, there exists only one combination of pressure and termperature when hydrates will be in equilibrium with the gas phase and aqueous phase.

For a given gas composition one can calculate hydrate formation conditions from the vapor-solid equilibrium constants for propane and carbon dioxide[21]. The contents of the cell are then kept at a pressure slightly above this predetermined pressure. The system is then supercooled by 10-12^{o}F. The equilibrium cell is then rocked till the hydrates are formed. Hydrate formation was accompanied by a drop in pressure. The temperature was then raised very slowly until a few crystals remained on the glass window. Due to dissociation of the hydrate

crystals, pressure increased with an increase in temperature. The crystals on the glass window were examined under a light source through a magnifying glass. When these crystals started decomposing, the temperature was lowered by 1-2^{o}F to recrystallize the hydrates. The temperature was again increased very slowly. The termperature and pressure, when these few new crystals dissociated, were noted. At this time a sample of the equilibrium gas phase was taken in the gas burette and analyzed.

The critical temperatures of carbon dioxide and propane are 87.8^{o}F and 206.0^{o}F respectively. Since the experimental temperatures were lower than these critical temperatures, these components will liquify in the L_2 phase at certain pressures. To obtain these conditions, the contents of the cell were compressed at about 75^{o}F until L_2 phase appeared. Depending upon the composition of the feed gas mixture, the composition of L_2 phase will vary from 100% propane to 0% propane. The temperature was then decreased and the equilibrium cell was rocked until a new hydrate phase appeared. At these conditions four phases, $H_{II}L_1L_2G$, were present.

A gas sample was prepared as described in part (i). Valve 2 was then opened and some mercury was pumped in until it appeared in the bottom of the cell. The valves 2, 4, 6, 7 were closed and the system evacuated for one hour. Valve 5 was

then closed and about 20 ccs of distilled water were taken into the cell at the top of valve 1. The valves 6, 1 were closed and some gas mixture was bled out at valve 4. The gas mixture was then fed into the cell. The valves 8 and 1 were closed and the cell connected to pressure gauge at valve 2. The mercury pump E was then manipulated until the desired pressure was read on the gauge. The temperature was set on the temperature bath. The equilibrium cell was then rocked until the hydrates were formed. The crystals on the surface were spread on the glass surface by tilting the cell. The temperature was increased slowly and these crystals on the glass window examined carefully until they just started to decompose. At this point, temperature was decreased slowly until some hydrates recrystallized on the glass surface. These crystals were then watched carefully through the magnifying glass when the temperature was being raised very slowly. When they started to decompose, pressure and temperature readings were noted. At this point, a sample of the gas phase was taken into a gas burette. The lines leading to the sampling point were evacuated prior to sampling the gas mixture. Care was exercised to see that the pressure did not fluctuate during the sampling procedure. The gas sample was allowed to stand in the burette for about 30 minutes and then analyzed on the gas chromatograph.

The system pressure was lowered and the above mentioned procedure repeated. For each mixture, it was found convenient to start with the quadruple point and then reduce the pressure for additional runs. Care was also taken to leave some crystals from the previous run to serve as seeding crystals for the next run. This facilitated hydrate formation. The water was changed for each gas mixture.

F. Experimental Difficulties

Since hydrate formation is a phenomenon similar to crystallization, it was observed that until crystallization has commenced, it is difficult to get hydrates to form even at pressures 200 to 300 psi higher than they will form when crystals are present. It was also noticed that alhtough most of the hydrates decompose readily, a small amount of hydrates persist for a considerable time. The crystals which fail to decompose, are either submerged in the water or completely covered by a water film. Particularly in the case of carbon dioxide it was found difficult to initiate hydrate formation. In this case, therefore, the subcooled contents of the cell were further cooled by sudden expansion of the charge.

EXPERIMENTAL RESULTS

A. Experimental Accuracy of the Results

Three variables measured in this work were pressure, temperature and composition. As the method used for determining initial hydrate formation conditions was visual, the results might involve some personal errors also. These personal errors were minimized by repeating the procedure in the neighbourhood of hydrate formation conditions. The use of a magnifying glass also facilitated visual observations.

The errors in the temperature measurements were limited to the errors of the sensing device and the measuring device. The iron-constantan thermocouple used for this work was calibrated with a standard mercury-in-glass thermometer at the ice-point and room temperature of 72°F. A linear correction was applied to the voltages and corresponding temperatures read from the potentiometer conversion tables. The potentiometer could read voltage difference equivalent to ±0.15°F.

The pressure gauge readings were corrected for level differences. The minimum gauge reading was 2 psi.

The chromatographic results were normalized on the prorata basis. The observed values of mole percentages of each component added to (100±3)%.

B. Propane-Water System

Experimental results for the initial hydrate formation conditions for the propane-water system are tabulated in Table I and Table II. The results are plotted in Figure 4. Investigations of other workers at similar conditions are reported in Table IV and compared with this work in Figure 4. The present measurements are in good agreement with those of other investigators.

The range of pressure (25-80 psia) and temperature (32-42.3°F) in which HL_1G equilibrium for C_3H_8-H_2O system persists is quite narrow. The three phase HL_1G equilibrium is terminated at the quadruple point, observed at T = 42.3°F and P = 80.0 psia. The vapor pressure curve for pure propane is shown in Figure 4, to give an idea of the approximate position of the HL_2G and L_1L_2G phase equilibria.

C. Carbon dioxide - Water system

Villard[53] was the first investigator to work on this binary system in three phase HL_1G equilibrium. Later Unruh and Katz[52] published their results for the system CO_2-CH_4-H_2O which included their experimental observations for the binary CO_2-H_2O system.

Experimental results of this work are tabulated in Table I and Table II, while those of other workers are reported in Table III. These are plotted on a semi-log graph in

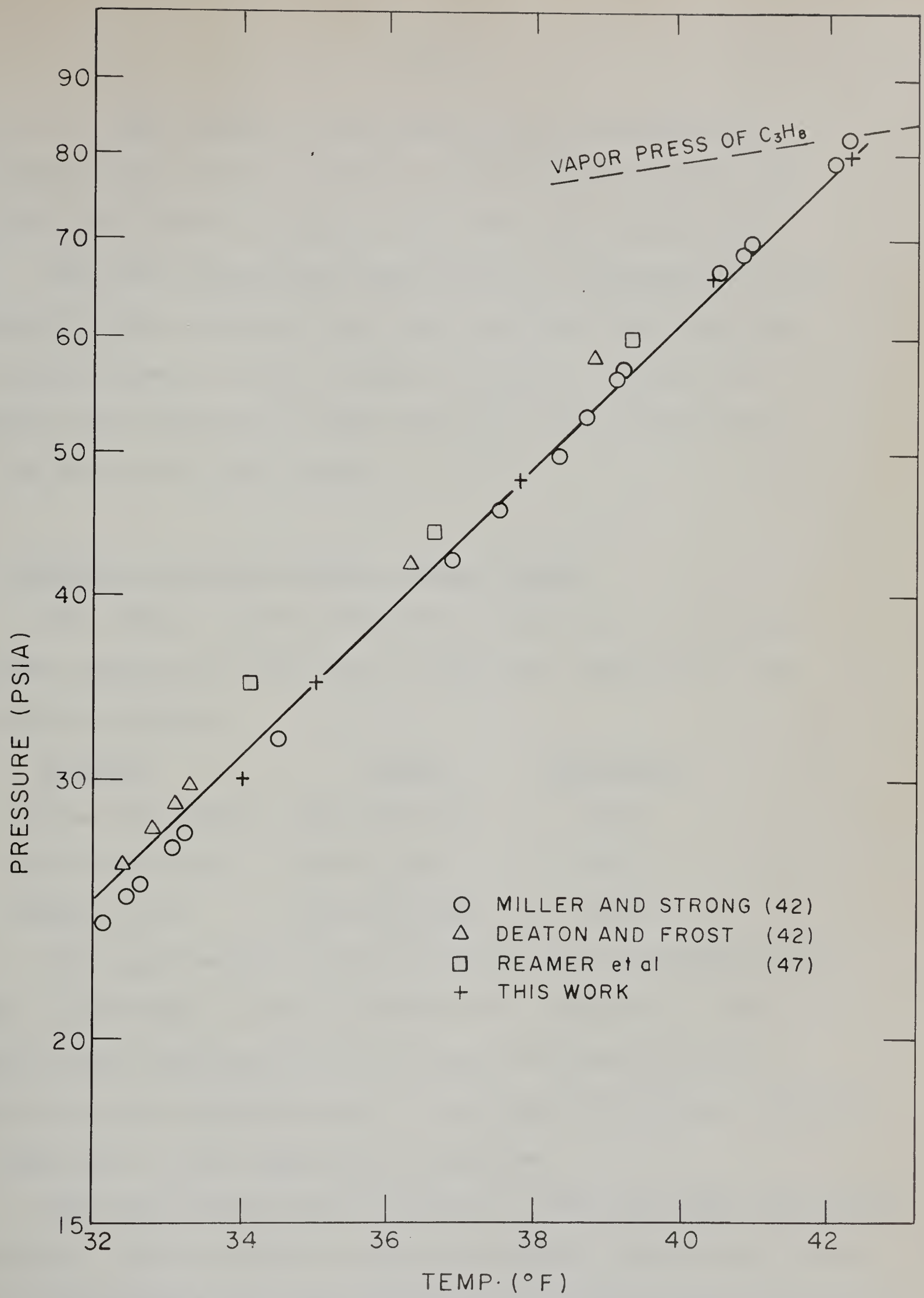

FIG. 4 COMPARISION OF EXPERIMENTAL DATA FOR $H_{II}L_1G$ EQUILIBRIUM FOR C_3H_8 - H_2O SYSTEM

Figure 5. The results of this work are in satisfactory agreement with Unruh's results, but Villard's observations reported in 1894 do not agree with the more recent data.

The three phase HL_1G equilibrium is terminated at the quadruple point found in this work at 50.3°F and 648 psia. The vapor pressure curve of CO_2 is shown on Figure 5 to indicate the location of HL_2G and L_1L_2G phase equilibria of the binary CO_2-H_2O system.

D. Propane - Carbon dioxide - Water system

The initial hydrate formation conditions of ternary systems containing either CO_2 or C_3H_8 are reported by the following workers:

	Authors	System	Reference
1.	Deaton and Frost	CH_4-C_3H_8-H_2O	(10)
2.	Unruh and Katz	CH_4-CO_2-H_2O	(52)
3.	Reamer et al	C_3H_8-C_3H_6-H_2O	(40)

The experimental results of this work are tabulated in Table I and Table II and are depicted in Figure 6. The compositions indicated in this figure are those of the equilibrium gas samples taken at the point of hydrate formation, as described in the experimental program.

The three phase equilibrium for a ternary system generates a surface. This surface is made of constant composition lines, each representing HL_1G equilibrium for the particular composition

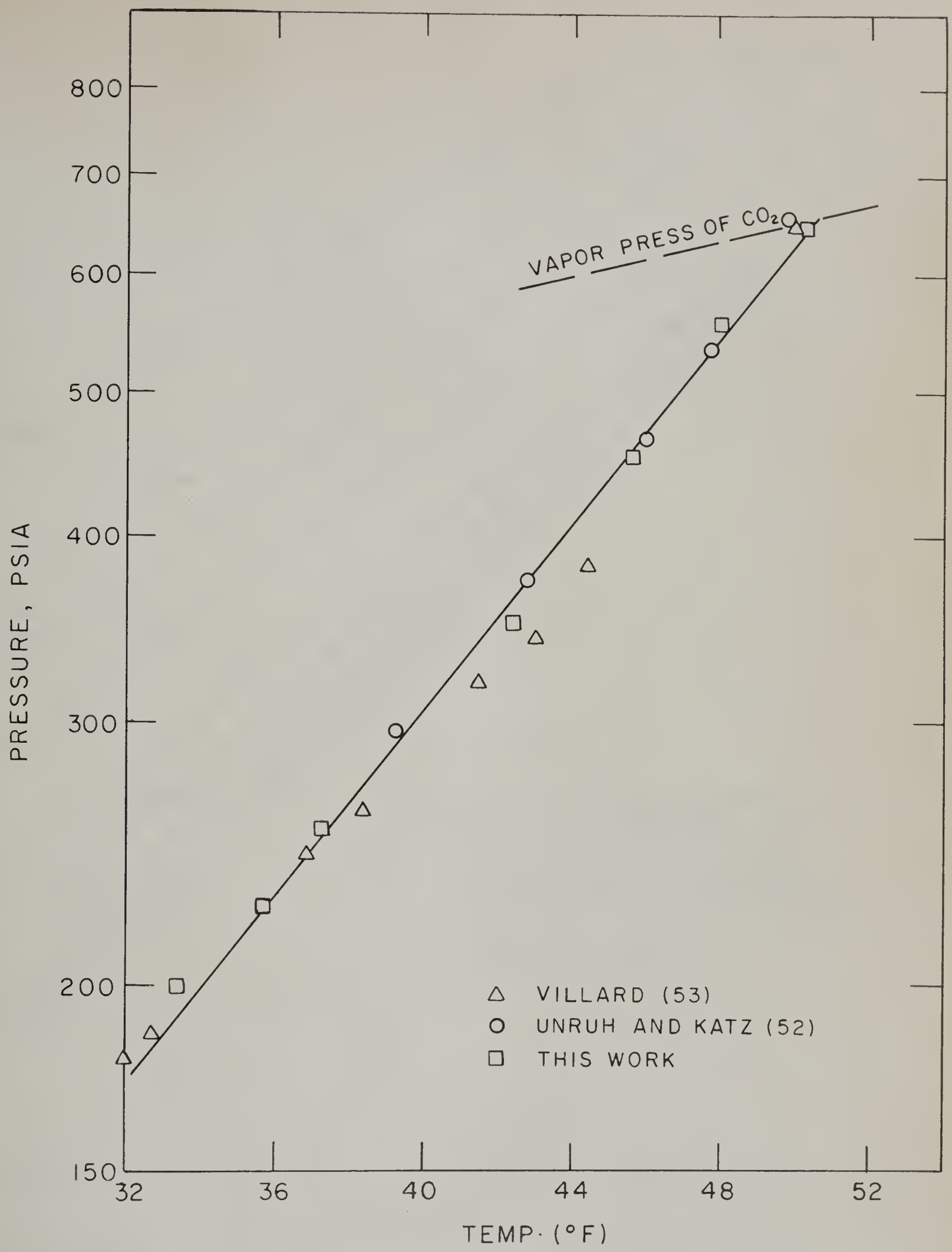

FIG. 5 COMPARISION OF EXPERIMENTAL DATA FOR THREE PHASE $H_I L_1 G$ EQUILIBRIUM FOR CO_2-H_2O SYSTEM

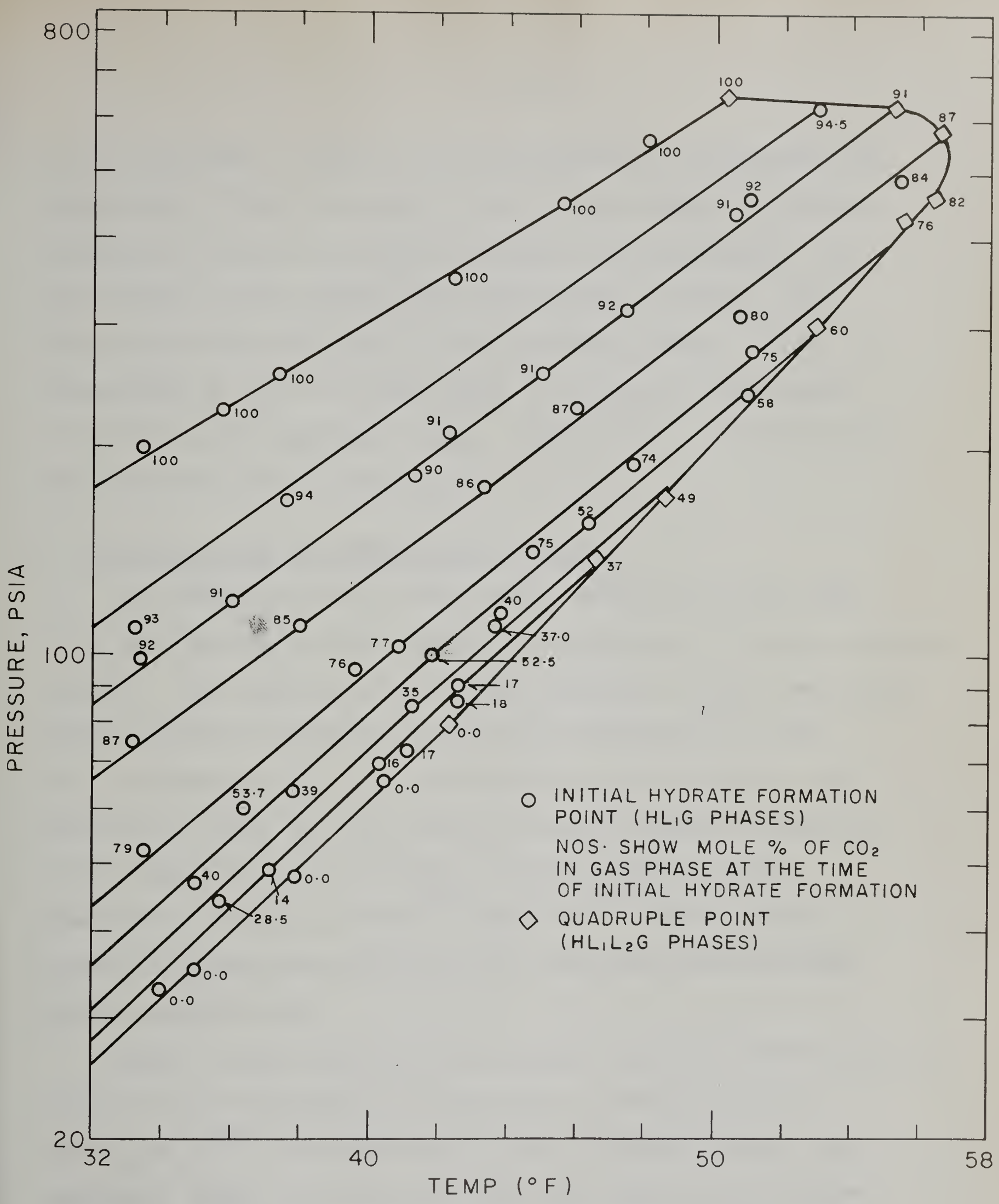

FIG·6 PRESSURE TEMPERATURE DIAGRAM OF THE SYSTEM $CO_2-C_3H_8-H_2O$ IN HL_1G AND HL_1L_2G PHASE EQUILIBRIA

of the gas phase. Since it is not possible to manipulate the composition of the gas phase at the initial hydrate formation conditions, the points shown in Figure 6 are scattered. The lines drawn in this region are approximately located. All these lines are terminated at the quadruple locus. It is interesting to note the occurrence of a maximum temperature of 56.7°F in the quadruple locus. There exist no Structure II hydrates beyond this temperature.

E. Discussion of the Experimental Results

The general trend of the results obtained in this work is in good agreement with similar investigations of other research workers. The addition of the heavy component (C_3H_8) lowers the initial hydrate formation pressure and temperature of the light component (CO_2). At the freezing point of water, the addition of about 10% C_3H_8 changes hydrate formation pressure of CO_2 from 175 psia to 85 psia. Similar effects were observed by Deaton and Frost[9] and Otto[32] during their studies on propane-methane-water and propylene-methane-water systems respectively.

Other ternary systems having phase behaviour characteristics similar to the CO_2-H_2O-C_3H_8 system are H_2S-$CHCl_3$-H_2O and H_2S-CCl_4-H_2O[56]. The quadruple locii of these systems look remarkably alike. The points on the four phase HL_1L_2G locus are the points of intersections of the three phase branches

HL_1G, HL_2G, HL_1L_2, L_1L_2G for a particular fixed gas composition. The branches HL_2G and L_1L_2G are located below the vapor pressure curve for the gas mixture of the same composition. From the available data[37, 39] on the system CO_2-C_3H_8, it was possible to draw dew point pressure-temperature curves for various compositions. These curves are shown in Figure 7 along with the quadruple locus and three phase HL_1G lines for the ternary CO_2-C_3H_8-H_2O system. The three phase lines in Figure 7 are located approximately due to the scatter in the points, as shown in Figure 6. By this method, the shape of the quadruple locus can be defined approximately.

The slope of a univariant phase equilibrium branch, plotted on a P-T plane, is given by the Clapeyron equation,

$$\frac{dP}{dT} = \frac{\Delta H}{T \cdot \Delta V} \qquad (15)$$

This thermodynamic identity is valid irrespective of how the compositions of the phases change along the equilibrium line. The quantities ΔH and ΔV denote the changes in the enthalpy and volume accompanying the phase transformation along the univariant equilibrium considered at constant P and T.

Approximately, $\Delta V = zRT/P$ (16)

Substituting equation (16) in (15) and rearranging,

$$\frac{d \ln P}{dT} = \frac{\Delta H}{z R T^2} \qquad (17)$$

Thus when ln P is plotted against T on a semi-log graph, the slope of this line is given by the right hand side of

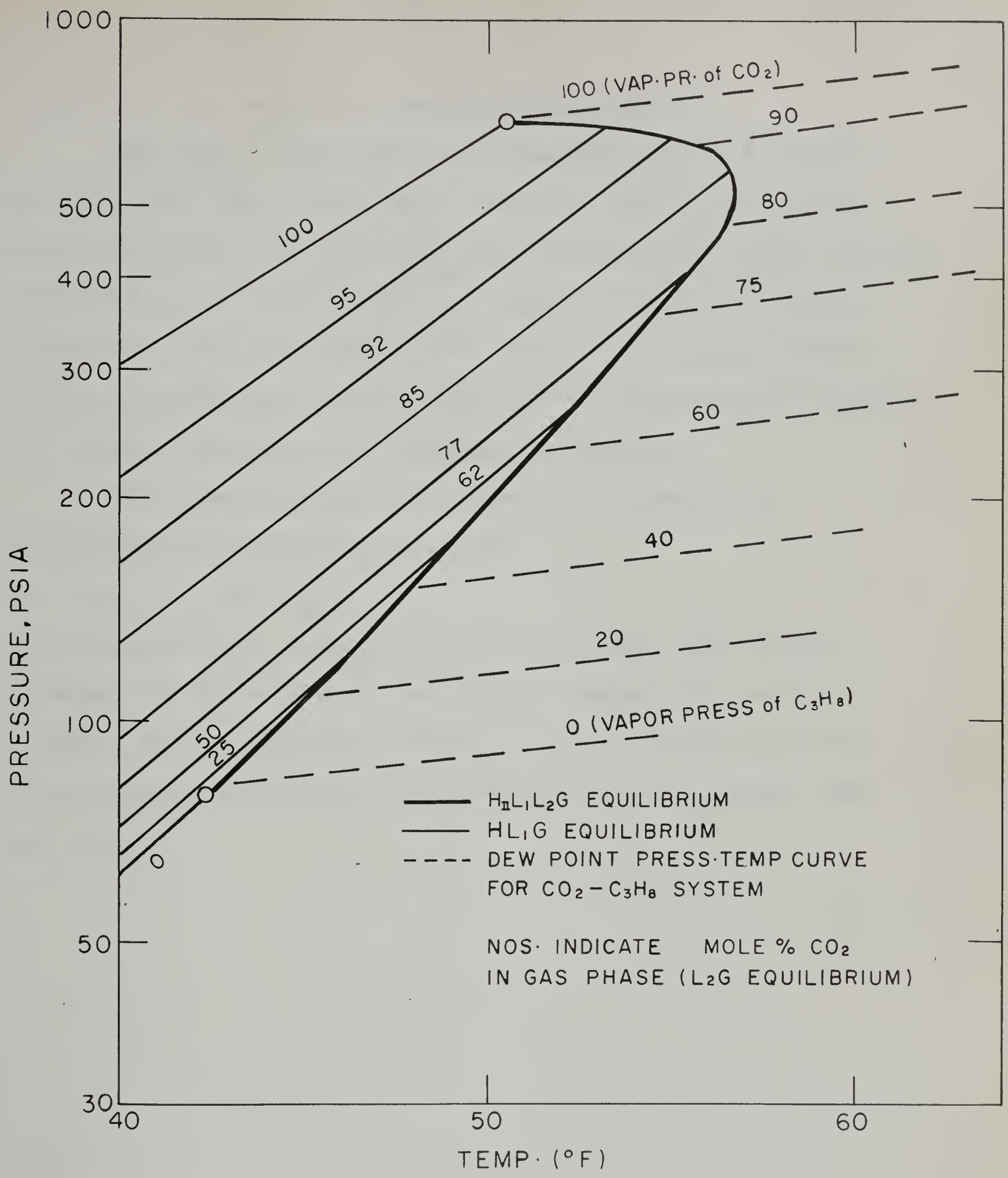

FIG·7 FOUR PHASE - $H_{II}L_1L_2G$ - LOCUS FOR $CO_2 - C_3H_8 - H_2O$ SYSTEM

equation (17), namely by the quantity ($\Delta H/zRT^2$).

The slope of the HL_1G curve for the C_3H_8-H_2O system is greater than that of the HL_1G curve for the CO_2-H_2O system. This is evident from the fact that ΔH value for carbon dioxide hydrates is 14.4 k-cal/mole[56], while the same for propane hydrates is 32.0 k-cal/mole[56]. This can also be deduced from the knowledge that the $\Delta\mu$ value for Structure II hydrates is greater than that for Structure I hydrates.

The transformation along the four phase HL_1L_2G equilibrium may be represented by,

$$L_1 + L_2 + G \longrightarrow H_{II}$$

The slope of this univariant quadruple phase equilibrium changes its direction at the maximum temperature point. A tangent moving along this locus will have maximum slope at this maximum temperature point beyond which H_{II} phase does not exist.

THEORETICAL RESULTS

A. Potential Models for Non-Spherical Molecules

Various potential functions have been proposed to account for the non-spherical shape of molecules like CO_2. The parameters of such a potential function could not be computed from first principles. They are customarily obtained from some macroscopic property. Of these, the second virial coefficient itself has been used most conveniently. Consequently the experimental information on the second virial coefficient of various molecules was collected to evaluate parameters.

A considerable improvement over the Lennard-Jones potential has been suggested by Kihara[38] who replaced the point center model for a molecule by an impenetrable core whose dimensions are suggested by the geometry and intermolecular distances of the molecule. Corner[7] proposed a four-center model for long molecules like CO_2 and C_3H_8. When these models were used to predict the dissociation pressures of gas hydrates, the discrepancy was quite pronounced. It was, therefore, concluded by McKoy[29] that the dissociation pressures are more sensitive to the parameters of the potential functions than are second virial coefficient data. The parameters for CO_2 and C_3H_8 are tabulated in Table V.

There is a unique set of parameters for a given molecule. They could, therefore, be computed by fitting the observed value of hydrate formation pressure and temperature

at a point on the HL_1G equilibrium curve. These values of (ε/k) and (σ) for CO_2 and C_3H_8 were used to calculate the rest of the pressures and temperatures along the three phase (HL_1G) equilibrium. The method of calculating these potential parameters is described in Appendix D. The values obtained by this procedure are,

Molecule	(ε/k), °K	(σ), Å
CO_2	148	3.96
C_3H_8	278	4.80

B. Langmuir Constants

The values of Langmuir constants by equation (3) are dependent on the parameters σ and ε/k which in turn are characterized by the potential model used. The parameters in Table V were used to calculate C_k values of CO_2 and C_3H_8 molecules. The procedure for calculation of Langmuir constants is shown in Appendix C.

Langmuir constants for C_3H_8 are plotted as a function of temperature in Figure 8 and Figure 9. It is interesting to notice the influence of change of the value of σ from 4.90Å (Curve B of Figure 9) to 5.50Å (Curve B of Figure 8), keeping (ε/k) constant at 228°K. A similar effect is brought about due to the change in (ε/k) values at constant (σ) value, as shown by Curve A of Figure 8 and Figure 9. When (σ) is increased by 89% at constant (ε/k) = 228°K the Langmuir

CURVE	(ε/k)°k	(σ), Å	REF.
A	515·14	4·80	(38)
B	228·00	5·50	(7)

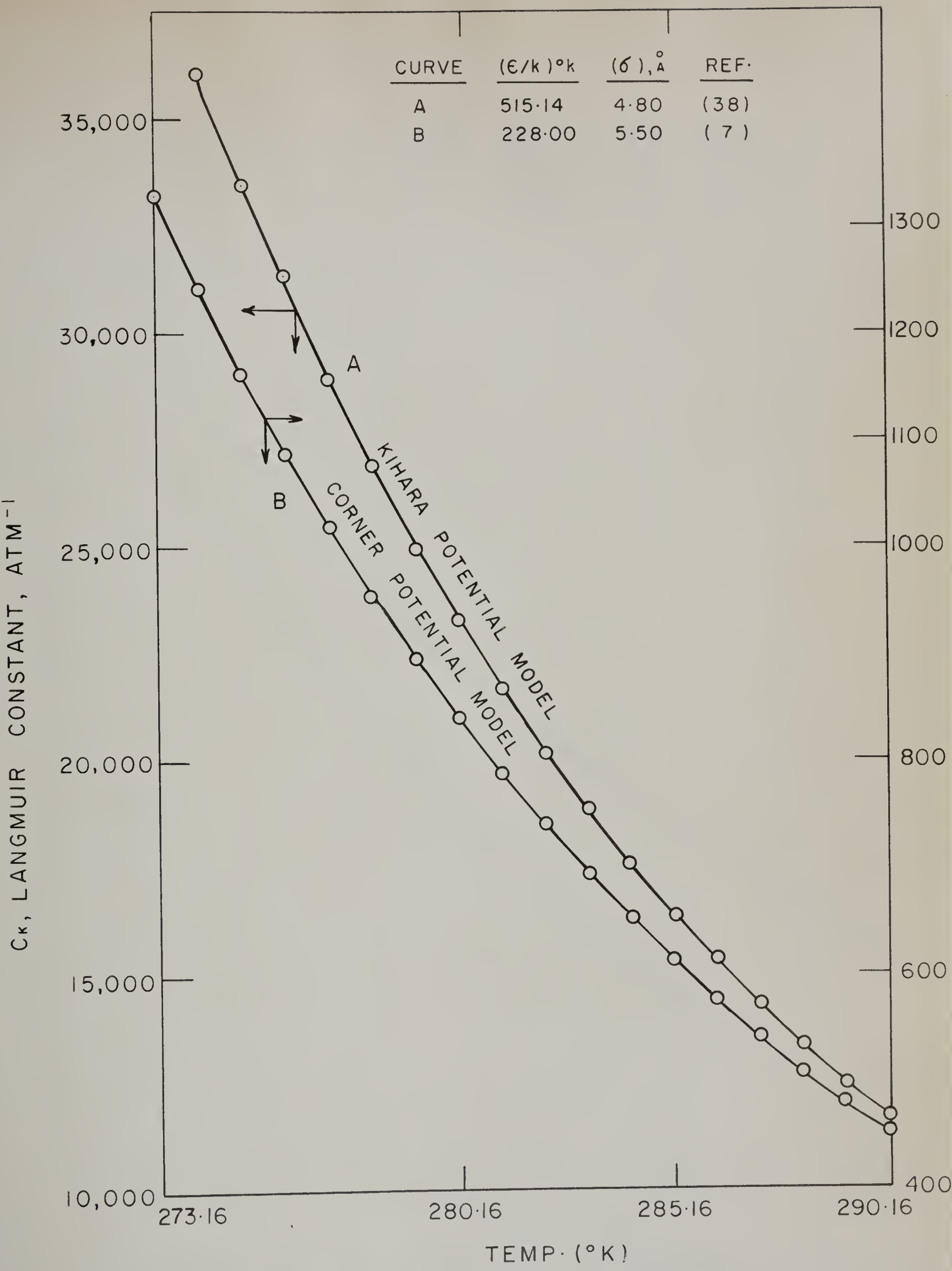

FIG·8 LANGMUIR CONSTANT FOR PROPANE MOLECULE IN STRUCTURE II HYDRATES, LARGE CAVITY

CURVE	(ϵ/k)°k	(σ), Å	REF.
A	278·0	4·80	THIS WORK
B	228·0	4·90	(18)

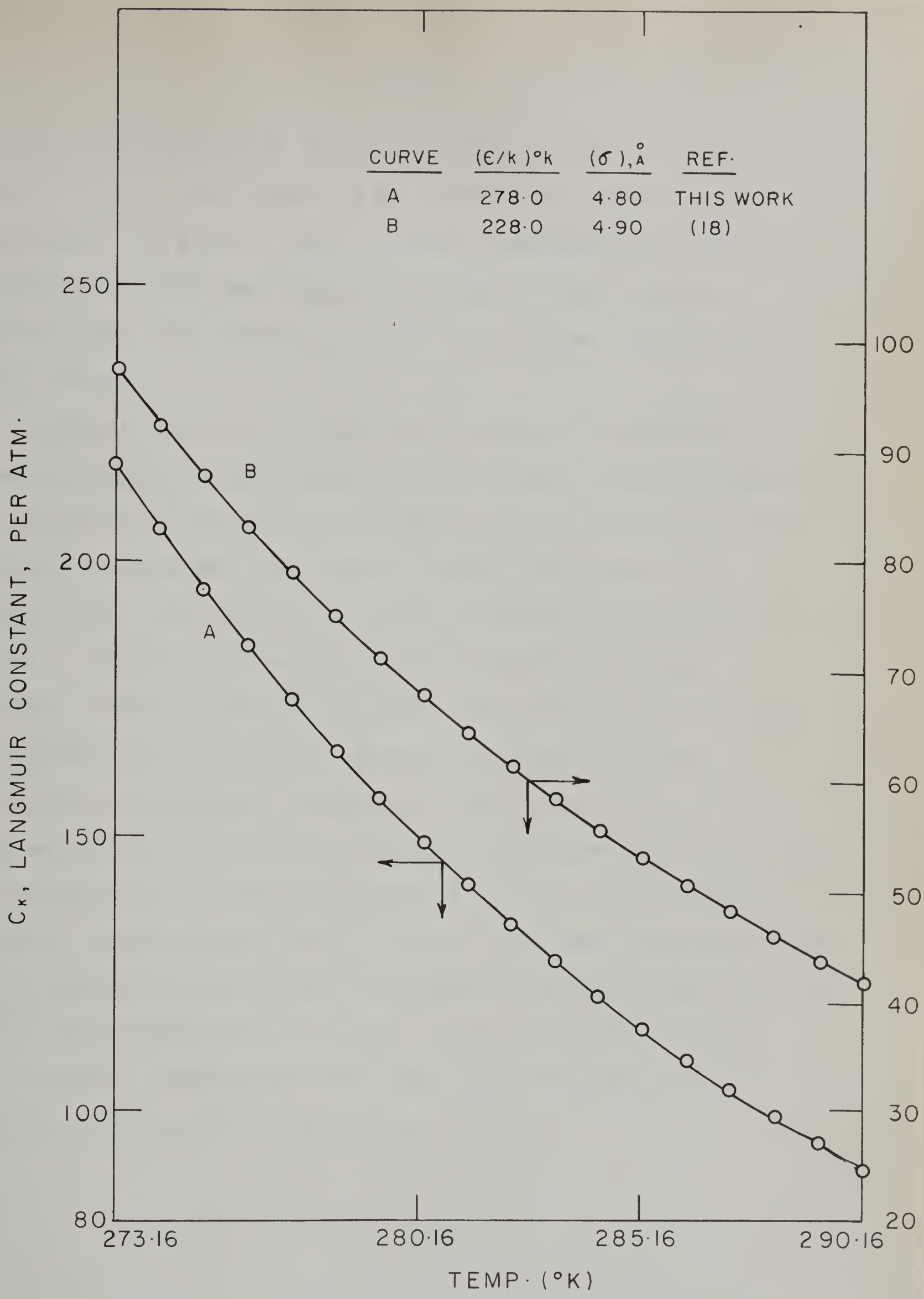

FIG·9 LANGMUIR CONSTANT FOR PROPANE MOLECULE IN STRUCTURE II HYDRATES, LARGE CAVITY

constant increased by an average of 7.85% over the temperature range of 0-17°C. But when (ε/k) values were raised by 54% at constant σ = 4.80 Å, the C_k values increased by an average of 0.62% over the same temperature range. Thus Langmuir constants are more sensitive to the (σ) values than to the (ε/k) values.

Langmuir constants of the CO_2 molecule in Structure I are shown in Figure 10 and Figure 11 for various potential models. For the models reported in the literature, C_k values in large cavities are smaller than those in small cavities at all temperatures. For the set of values obtained in this work, C_k values in large cavities are greater than those in small cavities. This can be explained by equation (2) which relates the probability of finding a molecule in large or small cavities to its Langmuir constants. To have y_{k2} y_{k1}, for a gas molecule in Structure I hydrates, one must have, C_{k2} C_{k1}. The probability of finding a molecule in the large cavities is obviously greater than that of finding the same molecule in the small cavities of Structure I hydrates. The same trend was also observed by Marshall[26] for CH_4, A and N_2 in Structure I.

Langmuir constants of CO_2 and C_3H_8 are tabulated in Table VI and Table VII respectively.

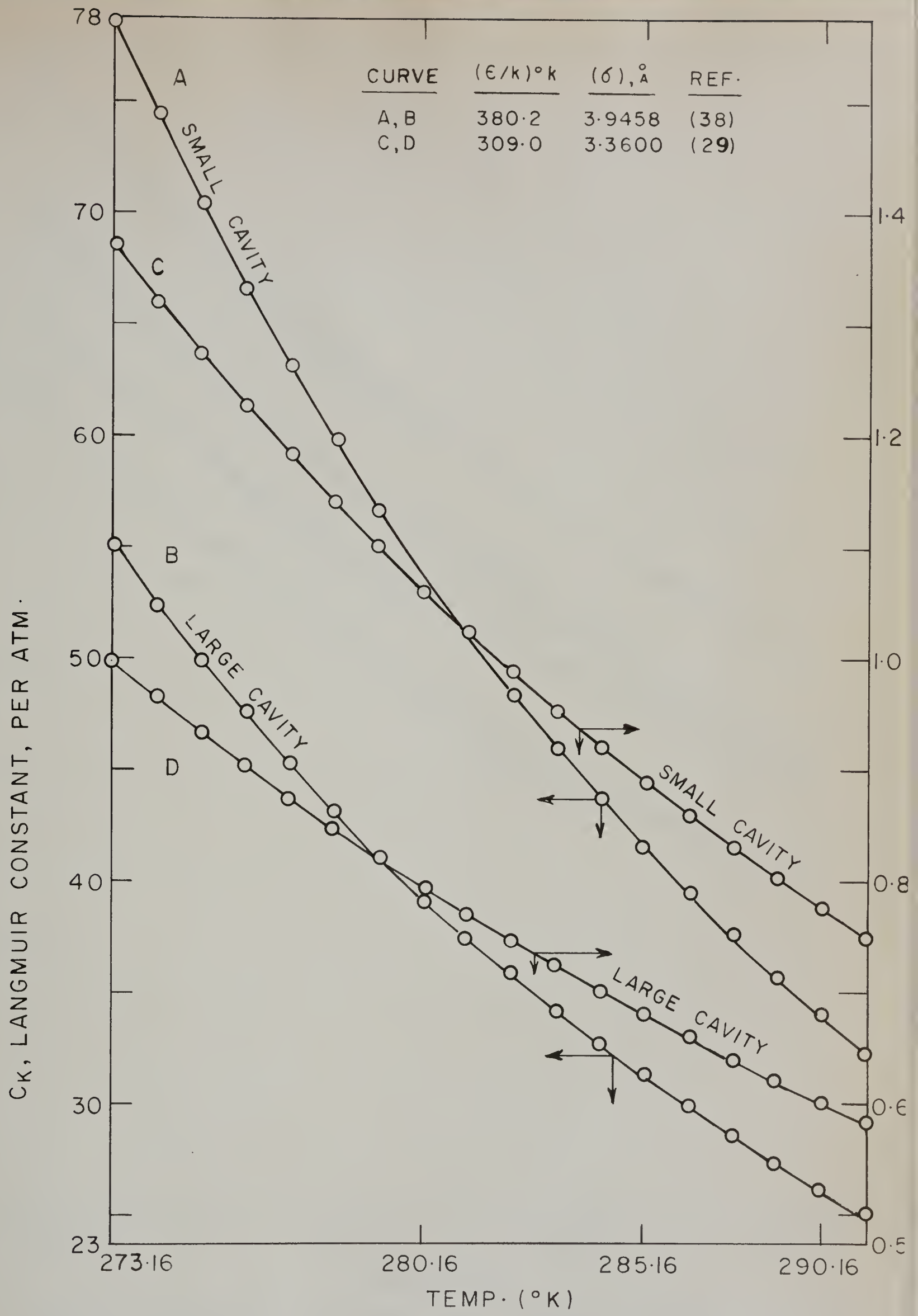

FIG·10 LANGMUIR CONSTANTS FOR CARBON DIOXIDE MOLECULE IN STRUCTURE I HYDRATES

CURVE	(ϵ/k) °k	(σ), Å	REF.
A, B	148·0	3·96	THIS WORK
C, D	198·0	3·57	(18)

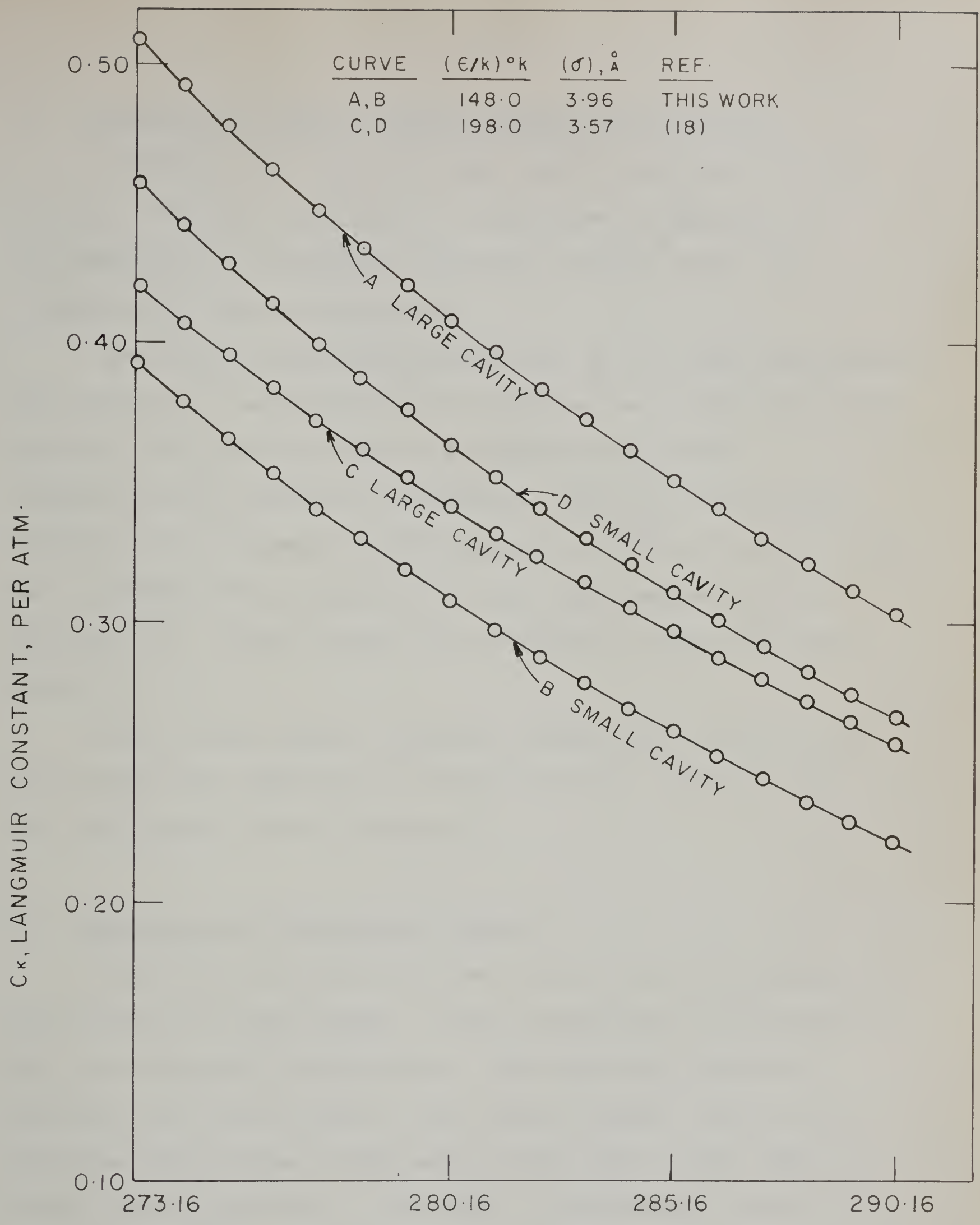

FIG. II LANGMUIR CONSTANT FOR CARBON DIOXIDE MOLECULE IN STRUCTURE-I HYDRATES

C. Prediction of Initial Hydrate Formation Conditions

Equations (12) and (14) were used to calculate initial hydrate formation conditions, as described in Appendix E. In addition to the Langmuir constants, values of $\Delta\mu'$ are required for these calculations.

The chemical potential difference $\Delta\mu'$ for HL_1G equilibrium for Structure I and Structure II hydrates were calculated from equation (14) using methane and sulfur hexafluoride respectively as reference components. Data for the methane hydrate were obtained from Shozaburo et al[46] and those for SF_6 were computed using equation (12) and experimental data of Sortland[48]. These values are tabulated in Table VIII and Table IX.

The initial hydrate formation conditions predicted by this method are tabulated in Table X and are compared with the experimental data in Figure 12.

D. Discussion of Theoretical Results

The solid solution theory was limited by the assumptions made during its development. These assumptions restricted the size and shape of the molecules. Non-spherical molecules like CO_2 will not be free in the entire cavity. When such a molecule comes close to the wall of its cage it will have to orient itself parallel to this wall. Furthermore, some of the cavities are somewhat oblate in shape, and thus the rotations

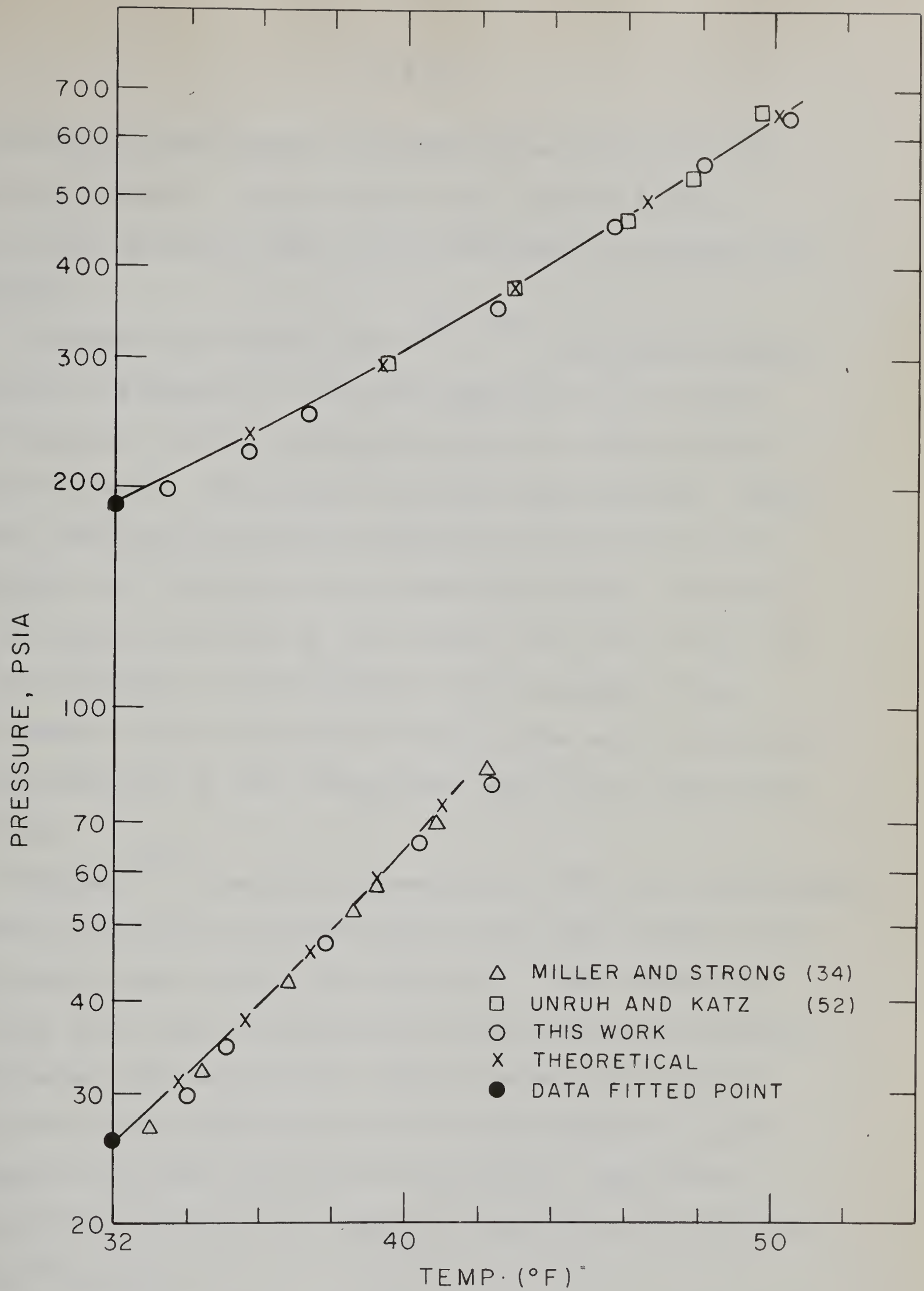

FIG. 12 COMPARISION OF EXPERIMENTAL AND THEORETICAL RESULTS FOR CO_2-H_2O AND C_3H_8-H_2O SYSTEMS IN HL_1G EQUILIBRIUM

of relatively large and/or non-spherical molecules may be seriously hindered. These effects will predict higher dissociation pressures than those calculated by assuming free rotations.

Platteeuw and van der Waals[56, 57] calculated Langmuir constants of propane at -3°C using equation (2), in which they obtained y values for SF_6 molecules and dissociation pressure from the experimental data for C_3H_8 hydrates. This implies that the equilibrium composition of the hydrate is independent of the nature of the guest molecules. Provided that the guest molecules do not distort the host lattice and that the pressure is low enough for the variation of $\Delta\mu$ with pressure to be negligible, the $\Delta\mu$ value will be constant for any molecule, at that temperature and for the particular structure.

Marshall[26] computed parameters (σ, ε/k) for the methane molecule by fitting different sets of (σ, ε/k) values to the experimental data at more than one point. The combination (σ, ε/k) which gave a minimum mean square deviation from the experimental data was chosen. The parameters for propane calculated by the method proposed in this work are in good agreement with those calculated by Marshall. The Corner potential was the one which gave C_k values close to the values used in this work.

To account for the non-ideal behaviour of CO_2 and C_3H_8, fugacities were used in all the calculations. The initial

hydrate formation conditions are sensitive to the parameters (σ) and (ε/k) because these parameters determine the Langmuir constants which at a given temperature influence dissociation pressures according to equation (12). It was observed in general that the increase in C_k values shifted the HL_1G curve down on the pressure-temperature plane, and vice versa.

The use of methane and sulfur hexafluoride as reference components proved very helpful. This approach assumes that the guest molecules do not distort the host lattice. This assumption was shown to be a very good approximation by McKoy[29].

The agreement between the predicted hydrate formation conditions and the experimental observations, as shown in Figure 12, is within 6%. The slope of the theoretical HL_1G equilibrium curve increases with pressure and temperature. This can be explained by equation (17). It was found that compressibility factor z decreases along the HL_1G equilibrium curve, with the increase in pressure and temperature. It can be intuitively said that the difference in the specific heats of the products and reactants is positive because the products (hydrates) are solids while the reactants are liquid and gaseous. Thus, by Kirchoff's law, ΔH will increase with the increase in temperature, assuming it to be independent of the change in pressure. The change in the T^2 term, where T is absolute temperature, is quite small. For these reasons, $(\Delta H/z)$ will increase with temperature and hence the slope of HL_1G equilibrium increases with the rise in pressure and temperature.

CONCLUSIONS

1. The three phase (HL_1G) equilibrium for the binary CO_2-H_2O system was determined in the temperature range 32°F to 50.3°F. The quadruple point for this system was observed at T = 50.3°F and P = 648 psia.

2. The binary system C_3H_8-H_2O was studied in its HL_1G equilibrium from 32°F to 42.3°F and its four phase (HL_1L_2G) point was found at T = 42.3°F and P = 80 psia.

3. The three phase equilibrium conditions for the ternary CO_2-C_3H_8-H_2O system were determined at different compositions. The quadruple locus for this ternary system was investigated. The maximum temperature point was observed in this quadruple (HL_1L_2G) locus at T = 56.7°F.

4. The parameters for the potential function of CO_2 and C_3H_8 computed in this work were found to be,

   Carbon dioxide: $(\sigma) = 3.96$ Å

   $(\varepsilon/k) = 148.0$ °K

   Propane: $(\sigma) = 4.80$ Å

   $(\varepsilon/k) = 278.0$ °K

5. The predicted initial hydrate formation conditions for CO_2-H_2O and C_3H_8-H_2O systems in HL_1G equilibrium agreed satisfactorily with the experimental data. Thus, the solid

solution theory was found to be valid for the three phase (HL_1G) equilibria of systems containing non-spherical molecules like CO_2 and C_3H_8.

AREAS FOR FUTURE WORK

1. To verify the shape of the P-T diagram of the CO_2-C_3H_8-H_2O system, some pressure-composition envelopes may be obtained experimentally. Such a study may also prove the coexistence of the two solid phases H_I and H_{II}. Such pressure-composition data may also be used to test the validity of the solid solution theory for the HL_1G equilibrium.

2. To avoid the trial and error procedure in calculating parameters σ and ε/k, attempts may be made to fit the data at two points and solve the simultaneous equations for two unknowns.

3. With these parameters, Langmuir constants may be computed for each hydrate former. These calculations may be compared with the published data on various hydrates. One may theoretically calculate the vapor-solid equilibrium constants and pressure-composition envelopes at desired temperatures and the pressure-temperature diagrams for multi-component systems.

4. With these procedures, one may evaluate the selectivity of the hydrate phase for a particular component compared to its concentration in the equilibrium gas phase. These calculations may decide upon the possibility of using the hydrate formation process for separation of multi-component mixtures.

APPENDIX A

CALIBRATIONS

A. Chromatograph Calibrations

A gas chromatograph, model K-2 supplied by the Burrell Corporation, was used to analyze the mixtures of carbon dioxide and propane. Separation of both components was satisfactory, using the following column and conditions:

Column: 250 cms long, packed with 30-60 # mesh Fire Brick, coated with Apiezon M Grease, using Benzene as a solvent. The proportion used was 30 gms of Fire Brick to 7 gms of Apiezon M Grease.

Column Temperature:	40°C
Detector Current:	180 mA
Helium Rate:	25 ml/min
Sample volume:	0.875 ml
Residence time for CO_2:	2 mins
Residence time for C_3H_8:	3 mins

Samples of known composition were prepared in the gas burette and analyzed at the above conditions. Peak height of each component was plotted against its composition. Unknown samples were then tested and their compositions normalized on a prorata basis. The calibration curve is shown in Figure 13. This curve is on the basis of attenuation of 50. Accuracy of this calibration is within $\pm$ 3%. The analysis of lean samples is not very accurate because the peak height of the lean component was not very reliable.

FIG·13 CHROMATOGRAPH CALIBRATION FOR $CO_2 - C_3H_8$ MIXTURES

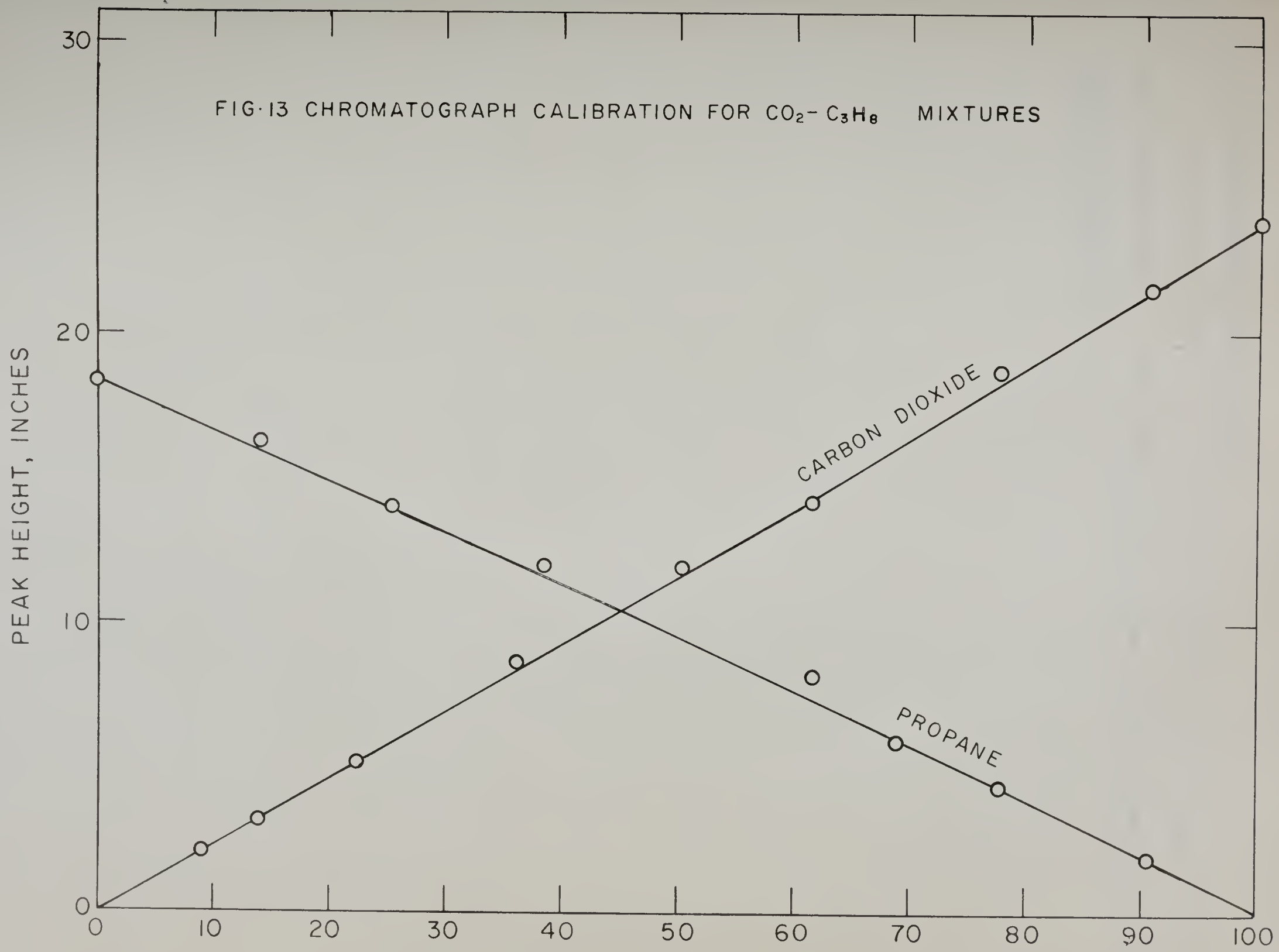

B. Thermocouple calibration

The thermocouple was standardized at the ice point and room temperature. The calibration curve after corrections is shown in Figure 14.

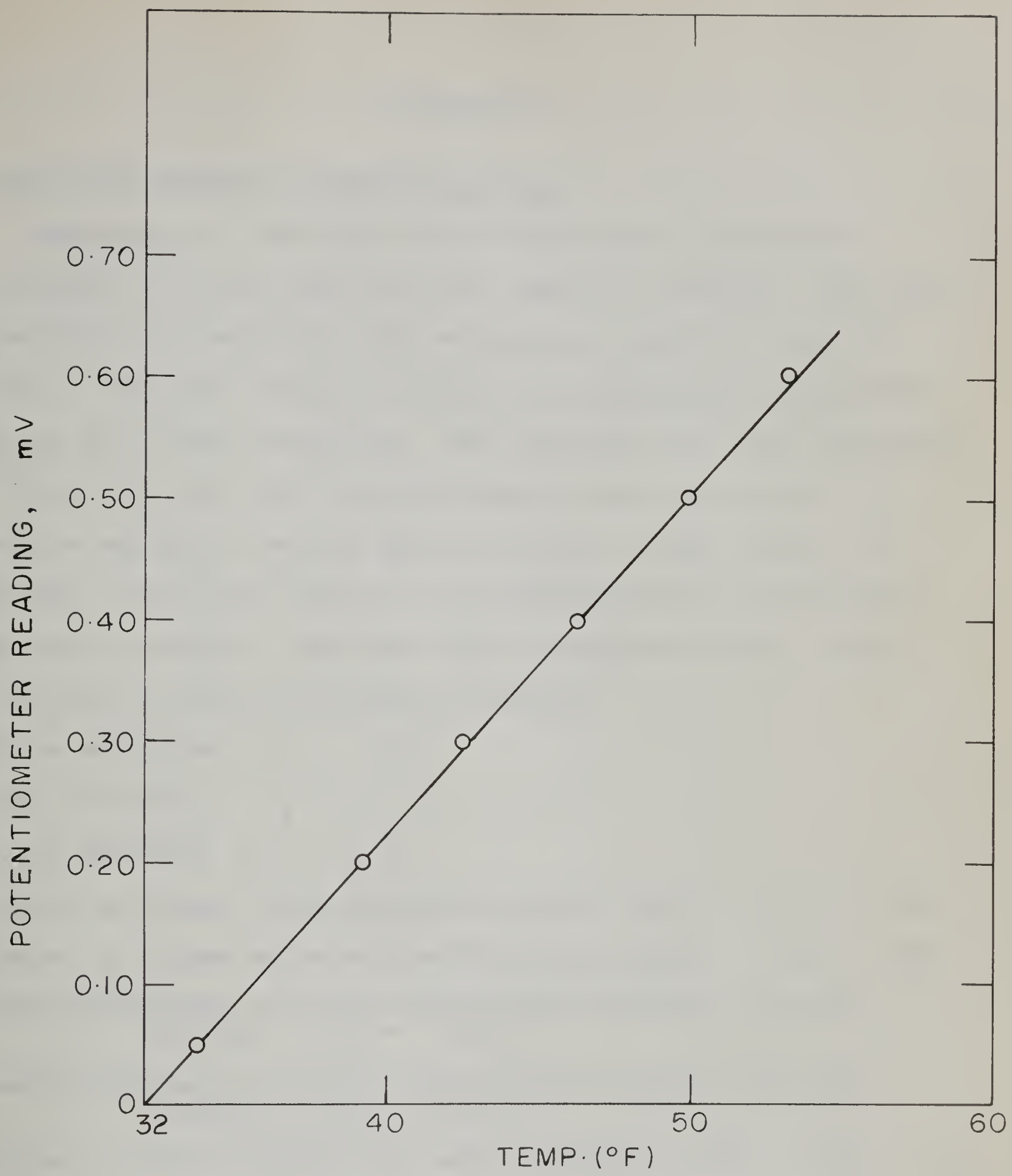

FIG·14 THERMOCOUPLE CALIBRATION CURVE

APPENDIX B

Structural Details of Hydrate Crystals

Structure I - The unit cell of Structure I contains 46 molecules of water which form two types of cavities. The small cavities are located at the vertices and center of the unit cell. The small cavity is formed by a pentagonal dodecahedral array of 20 water molecules. The remaining six water molecules in the unit cell form bridges between these dodecahedra in such a way that a second type of cavity, a large cavity, is formed. The large cavity is a tetrakaidecahedron having two opposite hexagonal faces and twelve pentagonal faces. Thus, Structure I has the following constants:

Water molecules = N_Q = 46

Small cavities = n_1 = 2

Large cavities = n_2 = 6

Number of oxygen atoms surrounding small cavity = z_1 = 20

Number of oxygen atoms surrounding large cavity = z_2 = 24

Average distance of oxygen atoms from the center of small cavity = a_1 = 3.95 Å

Average distance of oxygen atoms from the center of large cavity = a_2 = 4.30 Å

Number of small cavities per mole of water = $\nu_1 = \frac{n_1}{N_Q} = \frac{1}{23}$

Number of large cavities per mole of water = $\nu_2 = \frac{n_2}{N_Q} = \frac{3}{23}$

Free diameter of small cavities = 5.1 Å

Free diameter of large cavities = 5.8 Å

Chemical potential difference at 0°C = $\Delta\mu = \mu_Q^\beta - \mu_Q^\alpha$ = 167 cal/mole

Volume difference = $\Delta V = V^\beta - V^\alpha$ = 3.0 ml/mole

= $\Delta V' = V^\beta - V^L$ = 4.6 ml/mole

Structure II - The smaller cavities in this structure are distorted pentagon dodecahedra and the larger cavities are almost spherical. Various constants for this structure are:

Water molecules = N_Q = 136

Small cavities = n_1 = 16

Large cavities = n_2 = 8

z_1 = 20, a_1 = 3.91 Å, ν_1 = 2/17

z_2 = 28, a_2 = 4.73 Å, ν_2 = 1/17

Free diameter of small cavity = 5.0 Å

Free diameter of large cavity = 6.7 Å

$\Delta\mu = \mu_Q^\beta - \mu_Q^\alpha$ = 190 cal/mole at 0°C

$\Delta V = V^\beta - V^\alpha$ = 3.4 ml/mole

$\Delta V' = V^\beta - V^L$ = 5.0 ml/mole

The above values are quoted from reference 56.

APPENDIX C

Calculations of Langmuir Constants:

Langmuir's constant is defined by the equation,

$$C_{ki} = \frac{2\pi\, a_i^3\, g_{ki}}{k\,T} \exp\left[-\frac{W_{ki}(0)}{kT}\right]$$

where,

$$g_{ki} = \int_0^{1/4} \exp\left[\frac{Z_i\,\varepsilon}{k\,T}\left(-\frac{l(y)}{\alpha_i^4} + \frac{2m(y)}{\alpha_i^4}\right)\right] y^{1/2} \cdot dy$$

where,

$$l(y) = \left[(y^4 + 12y^3 + 25.2y^2 + 12y + 1) / (1 - y)^{10}\right] - 1$$

$$m(y) = \left[(1 + y) / (1 - y)^4\right] - 1$$

$$\alpha_i = (a_i / \bar{\sigma})^3 / \sqrt{2}$$

$$\bar{\sigma} = (\sigma_Q + \sigma_k) / 2$$

$$\varepsilon/k = (\varepsilon/k)_Q^{1/2} (\varepsilon/k)_k^{1/2}$$

$$\frac{W_{kj}(0)}{k\,T} = \frac{Z_i\,\varepsilon}{k\,T}\left[\frac{1}{\alpha_i^4} - \frac{2}{\alpha_i^2}\right]$$

To calculate the g_{ki}, "free volume", numerical integration by using Simpson's Rule was carried out on a digital computer IBM 7040. According to Simpson's Rule,

$$\frac{\quad}{\quad} \quad \frac{\quad}{\quad}$$

$$\int_a^b f(y) \cdot d\,y = \frac{h}{3}\left[y_o + 4\,(y_1 + y_3 + \ldots + y_{n-1}) + 2\,(y_2 + y_4 + \ldots y_{n-2}) + y_n \right]$$

The area under the curve is divided into n even number of slices, each of a width equal to h. In the present case, $a = 0$, $b = 1/4$, $y_o = 0$. The integrand decays as y increases and hence, it was found that $y_n = 0$. With these simplifications, Simpson's Rule becomes,

$$\int_o^{1/4} f\,(y) \cdot d\,y = \frac{2h}{3}\left[2\,(y_1 + y_3 + \ldots + y_{n-1}) + (y_2 + y_4 + \ldots + y_{n-2}) \right]$$

In this work the area was divided into 1024 parts when the values of g_k converged in the fifth decimal place.

The Langmuir constant is made up of three terms, namely

(i) $(2\pi\, a_i^3 / kT)$

(ii) g_{ki} and

(iii) $\exp\left[- \frac{W_{ki}(0)}{k\,T} \right]$

Term (i) is a volume term and is a constant for a given structure and cavity type. Term (ii) accounts for the free volume in a cavity. Term (iii) is an exponential function and hence is sensitive to the values of parameters σ and ε/k. As the value of σ increases, the Langmuir constant increases. A similar effect is observed due to an increase in the (ε/k)

values. These are evident in Figures 8 to 11. In all cases Langmuir constants decrease with increasing temperature.

APPENDIX D

Calculation of Parameters σ and ε/k

For the solid solution theory to be exact, there should exist a unique set of values of ε/k and σ of a gas molecule for all its data on hydrates. Once these values are determined, Langmuir constants could be calculated as a function of temperature.

The reported values of these parameters show large variations as shown in Table V. In order to fit these constants to the hydrate data, an attempt was made to force fit the experimental and calculated values of dissociation pressure at 0°C. As there are two unknowns, ε/k and σ, one of the two was assumed, and the other one adjusted by the iteratative method until the observed and calculated values of the dissociation pressure agreed. In this work σ was assumed for each gas molecule and (ε/k) adjusted until the two values of dissociation pressure matched.

The solubility data of carbon dioxide (19, 58, 59) and Propane (21, 24) were extrapolated into the hydrate region by Othmer's Plot[33]. Sulfur hexafluoride was found (14) to be negligibly soluble in water. Data for methane hydrates were obtained from Shozaburo[46, 47].

Carbon dioxide, (σ) and (ε/k)

Pure carbon dioxide grows in Structure I and occupies its large and small cavities.

From equations (12) and (14), we have,

$$\Delta\mu' = RT \left[\nu_1 \ln (1 + C_{k1} p_k) + \nu_2 \ln (1 + C_{k2} p_k) + \ln x_Q \right] \quad (12)$$

$$\Delta\mu' = \Delta\mu'_o + \Delta V' (P - P_o) \quad (14)$$

Selecting methane as a reference component, values of $\Delta\mu'_o$ and P_o were obtained from Kobayashi et al[46, 47]. In order to account for the nonideality of carbon dioxide, fugacities (p_k) were used in all the calculations. From experimental observations it was found that P = 172.0 psia at 0°C. Assuming σ = 3.96 Å, C_{k1} and C_{k2} were calculated for every iteratative value of (ε/k). Knowing the fugacity p_k at P = 172.0 psia and T = 0°C, and the solubility (x_Q), values of $\Delta\mu'$ from equation (12) were computed on the IBM 7040 computer for each iteration. This process of iteration was continued until $\Delta\mu'$ values from equations (12) and (14) matched. The parameters so determined for carbon dioxide were (σ) = 3.96 Å, (ε/k) = 148°K. The Langmuir constants using these parameters are shown in Figure 11.

Propane, (σ) and (ε/k)

Propane forms Structure II hydrates and enters the large cavities only.

From equations (12) and (14), we have,

$$\Delta\mu' = RT \left[\nu_2 \ln (1 + C_{p2} p_p) + \ln x_Q \right] \qquad (12)$$

$$\Delta\mu' = \Delta\mu'_o + \Delta V' (P - P_o) \qquad (14)$$

Sulfur hexafluoride was chosen as a reference component for Structure II hydrates. Pressure-temperature experimental data for SF_6 hydrates, as reported by Sortland[48] were used. Langmuir constants for the SF_6 molecule are given in Table IX. Using these values, $\Delta\mu'_o$ was calculated from equation (12) when $x_Q = 1.0$ because SF_6 is negligibly soluble in water. Assuming $\sigma = 4.80$ Å for the propane molecule, (ε/k) was determined by the iteratitive procedure, similar to the one described for carbon dioxide. Values of these parameters so obtained were $\sigma = 4.80$ Å and $(\varepsilon/k) = 278$ °K.

APPENDIX E

Prediction of Initial Hydrate Formation Conditions

With the best fitted values of parameters σ, ε/k for carbon dioxide and propane, as described in Appendix D, Langmuir constants were calculated as a function of temperature. (See Figures 9 and 11).

At a selected temperature, values of $\Delta\mu'$ can be calculated for each structure, at various total pressures P, from equation (12). At the same temperature, values of Langmuir constants are known. From solubility data, x_Q is determined at this temperature and various total pressures P. An iteratative procedure was set up for various values of the fugacity of the pure component at the same temperature and various total pressures P, to calculate $\Delta\mu'$ from equation (12). The iterations were continued until the values of the chemical potential difference calculated from equations (12) and (14) matched.

Results of such calculations are shown in Table VI, for CO_2-H_2O and C_3H_8-H_2O systems.

APPENDIX F

Tabulations

TABLE I

Experimental Data on Initial Hydrate Formation for CO_2-C_3H_8-H_2O System in Three Phase - HL_1G Equilibrium

Mole % CO_2 in Feed Gas	Pressure, psia	Temperature, °F	Mole % CO_2 in G-phase
100	200	33.4	100
	226	35.7	100
	255	37.3	100
	351	42.4	100
	454	45.6	100
	557	48.0	100
95	461	51.0	92.0
	317	47.4	92.0
	182	41.3	90.0
	120	36.0	85.0
	98	33.4	92.0
93	619	53.0	94.5
	440	50.6	91.0
	257	45.0	91.0
	211	42.3	91.0
	167	37.6	94.0
	118	33.2	93.0
91	490	55.4	84.0
	228	46.0	87.0
	175	43.3	86.0
	110	38.0	85.0
	75	33.2	87.0
82	278	51.1	75.0
	142	44.7	75.0
	95	39.6	76.0
	52	33.5	79.0
80	189	47.6	74.0
	103	40.8	77.0

Table I - (continued)

Mole % CO_2 in Feed Gas	Pressure, psia	Temperature, °F	Mole % CO_2 in G-phase
64	240	51.0	58
	155	46.3	52
	100	41.8	52.5
	60	36.5	57.8
46	115	43.8	40
	109	43.6	37
	84	41.2	35
	63	37.8	39
	47	35.0	40
29	86	42.6	18
	73	41.1	17
	44	35.7	28
15	93	42.7	17
	69	40.3	16
	49	37.1	14
0	66	40.4	0
	48	37.8	0
	35	35.0	0
	30	34.0	0

TABLE II

Experimental Data for Four Phase HL_1L_2G Equilibrium for CO_2-C_3H_8-H_2O System

Mole % CO_2 in Feed Gas	Pressure, psia	Temperature, °F	Mole % CO_2 in G phase
100	648	50.3	100
95	632	55.2	91
91	580	56.7	87
82	435	55.5	76
80	462	56.4	82
64	300	52.9	60
46	169	48.6	49
29	139	46.6	37
0	80	42.3	0

TABLE III

Experimental Data of Other Workers for CO_2-H_2O System in HL_1G Equilibrium

Authors	Pressure, psia	Temperature, °F
Unruh and Katz (52)	653	49.6
	535	47.7
	468	45.9
	375	42.8
	296	39.3
Maximum temperature for HL_1G equilibrium = 50.36°F		
Villard (53)	179.34	32.00
	186.69	32.86
	245.49	36.86
	263.13	38.48
	320.46	41.54
	342.51	42.98
	383.67	44.42
	651.21	50.00

TABLE IV

Experimental Data of Other Authors for

C_3H_8-H_2O System in the Three Phase HL_1G Equilibrium

Authors	Pressure, psia	Temperature, °F
Miller and Strong[34] (99.9% pure propane)	82.0	42.25
	79.5	42.07
	69.5	40.91
	68.5	40.82
	66.5	40.46
	57.0	39.20
	56.5	39.11
	53.0	38.66
	50.0	38.30
	46.0	37.49
	42.5	36.86
	32.0	34.52
	27.5	33.26
	27.0	33.08
	25.5	32.63
	25.0	32.45
	24.0	32.09
Deaton and Frost[34] (99.8% pure propane)	58.24	38.8
	42.22	36.3
	29.72	33.3
	27.97	33.1
	27.84	32.8
	26.28	32.4
Reamer, Selleck and Sage[40]	60.0	39.3
	44.2	36.6
	34.9	34.1

TABLE V

Values of Force Constant ε/k and

Molecular Parameter σ

Molecule	(ε/k), °K	(σ), Å	Source
Carbon dioxide	380.2	3.95	(38)
	309.0	3.36	(29)
	198.0	3.57	(18)
	148.0	3.96	This work
Propane	515.14	4.80	(38)
	228.00	5.50	(7)
	228.00	4.90	(18)
	278.00	4.80	This work
Sulfur Hexafluoride	200.9	5.51	(18)
Methane	150.55	3.66	(46)

TABLE VI

Langmuir Constants for CO_2 in Structure I Hydrates, Using (σ) = 3.96 Å, (ε/k) = 148 °K

Temperature, °C	C_k, small cavity, per atm.	C_k, large cavity, per atm.
0	0.3934	0.5095
1	0.3796	0.4933
2	0.3665	0.4778
3	0.3538	0.4629
4	0.3417	0.4486
5	0.3301	0.4347
6	0.3190	0.4214
7	0.3083	0.4086
8	0.2980	0.3963
9	0.2882	0.3844
10	0.2787	0.3730
11	0.2696	0.3620
12	0.2609	0.3513
13	0.2525	0.3411
14	0.2445	0.3312
15	0.2367	0.3217
16	0.2292	0.3125
17	0.2221	0.3036

TABLE VII

Langmuir Constants for C_3H_8 in Structure II

Hydrates, Large Cavity, Using (σ) = 4.80 Å, (ε/k) = 278 °K

Temperature, °C	C_k, per atmosphere
0	226.99
1	214.76
2	203.26
3	192.46
4	182.30
5	172.75
6	163.76
7	155.29
8	147.32
9	139.81
10	132.73
11	126.05
12	119.75
13	113.81
14	108.20
15	97.89
16	93.16
17	88.69

TABLE VIII

Chemical Potential of Methane

Hydrate in Structure I

P Total Press.,	f Fugacity,	T Temp.,	C_{M1} small cavity,	C_{M2} large cavity,	$\Delta\mu'$ cal per mole
26.0	24.5	273.16	0.2028	0.2175	172.3
68.0	59.2	282.90	0.1525	0.1690	231.1
136.0	106.2	289.00	0.1285	0.1450	275.1
204.1	148.3	292.30	0.1173	0.1332	301.4
272.1	191.0	294.40	0.1099	0.1257	322.0

TABLE IX

Chemical Potential of SF_6

Hydrate in Structure II

T, °K	P, psia	C_k, large cavity, atm^{-1}	$\Delta\mu'$, cal per mole
273.16	11.82	470.97	189.64
275.16	17.19	415.31	199.00
277.16	26.18	366.90	210.05
279.16	41.30	324.71	222.43
281.16	66.68	287.87	235.80
283.16	108.96	255.65	249.79
285.16	178.15	227.41	264.04
287.16	288.07	202.62	278.14
289.16	455.48	180.82	291.71
291.16	696.17	161.61	304.35

TABLE X

Calculations of Initial

Hydrate Formation Conditions

System	P, psia	T, °F
C_3H_8-H_2O	25.95	32.0
	31.21	33.8
	37.80	35.6
	46.76	37.4
	58.70	39.2
	74.28	41.0
CO_2-H_2O	191.1	32.0
	237.2	35.6
	293.5	39.2
	373.4	42.8
	496.1	46.4
	650.0	50.0

NOMENCLATURE

a_i	Cell radius of i type cavity
$\mathring{A}$	Angstrom unit
A, B	Hydrate forming components
C	Number of components
C_{ki}	Langmuir constant of k molecule in i type cavity
f	Fugacity
F	Number of degrees of freedom or free energy per mole
g_{ki}	Free volume of k molecule in i type cavity
G	Gas phase
ΔH	Enthalpy difference per mole
H	Hydrate phase or enthalpy per mole
h_{Ji}, h_{Ki}	Partition function of J (or k) molecule in i type cavity
I	Ice phase
k	Boltzmann's constant or conversion factor
L_1	Water rich liquid phase
L_2	Water lean liquid phase
N	Number of molecules
n	Number of moles, number of cavities
P	Pressure or number of phases
P_o	Total pressure of a reference component
p_J, p_k	Partial pressure of J (or k) component, fugacity when non-ideal behaviour
Q	Lattice former, water
R	Gas constant, hydrate former

r	Radial position
T	Absolute temperature
V	Volume
$\Delta V'$	Molar volume difference between β and L forms
x_k	Mole fraction of gas k in equilibrium with H and L_1 phases
x_Q	Mole fraction of water in L_1 phase
y_{ki}	Probability of finding k molecule in i type cavity
Y_k	Concentration of hydrate former k in H phase
Z	Number of oxygen atoms surrounding a cavity or compressibility
α	Stable modification of lattice former (ice or water) or dimensionless parameter of the cell geometry
β	Metastable modification of lattice former (empty lattice)
λ_k	Absolute activity of molecule k
ν_i	Cavities of type i per mole of Q
$6, \varepsilon/k$	Molecular parameter, force constant
$\Delta\mu$	Chemical potential difference per mole
$\phi_k(T)$	Molecular partition function

SUBSCRIPTS

g	Gaseous state
i	Type of cavity
J	Any component
k	Carbon dioxide, any component

l	Liquid state
M	Methane
o	Reference component
p	Propane, constant pressure
Q	Lattice former, water molecules
s	Solid state
T	Constant temperature

SUPERSCRIPTS

α	Crystalline stable form of lattice former
β	Metastable form of lattice former
L	Liquid stable form of lattice former
*	Chemical potential assuming ideal solution
'	Chemical potential difference assuming ideal solution behaviour

BIBLIOGRAPHY

1. Akers, W.W., Kelley, R.E., Lipscomb, T.G.; Ind. Eng. Chem., 46, 2535 (1954).

2. Barduhn, A.J., Towlson, H.E., Hu, Y.C.; A.J.Ch.E. Journal, 8, 175 (1962).

3. Barrer, R.M., Stuart, W.I.; Proc. Roy. Soc. (London), A243, 172 (1957).

4. Bond, D.C., Russell, N.B.; A.I.M.E. Trans., 179, 192 (1949).

5. Carson, D.B., Katz, D.L.; A.I.M.E. Trans., 146, 150 (1942).

6. Claussen, W.F.; J. Chem. Phy., 19, 259, 662, 1425 (1951).

7. Corner, J.; Proc. Roy. Soc. (London), A192, 275 (1948).

8. Deaton, W.M., Frost, E.M.; Oil and Gas Journal, 75, May 20 (1937).

9. Deaton, W.M., Frost, E.M.; Oil and Gas Journal, 170, July 27 (1946).

10. Deaton, W.M., Frost, E.M.; Bureau of Mines Monograph No. 8, U.S. Dept. of Int., (1946).

11. Forcrand, R. de; Compt. Rend., 134, 835, 991 (1902).

12. Forcrand, R. de; Compt. Rend., 135, 959 (1902).

13. Forcrand, R. de; Compt. Rend., 176, 355 (1923).

14. Friedman, H.L.; J. Am. Chem. Soc., 76, 3294 (1954).

15. Hammerschmidt, E.G.; Ind. Eng. Chem., 26, 851 (1934).

16. Hammerschmidt, E.G.; Oil and Gas Journal, 37 (52), 66 (1939).

17. Hammerschmidt, E.G.; Oil and Gas Journal, 61, May 23 (1940).

18. Hirschfelder, J.O., Curtiss, C.F., Bird, R.B.; "Molecular Theory of Gases and Liquids", John Wiley (1955).

19. International Critical Tables; vol. III, p. 255.

20. Jhaveri, J.M.; M.Sc. Thesis, University of Alberta (1963).

21. Katz, D.L., et al; "Natural Gas Engineering Handbook", McGraw-Hill (1959).

22. Knox, W.G., Hess, M., Jones, G.E., Smith, H.B.; Chem. Eng. Prog., 57, 66 (1961).

23. Kobayashi, R., Katz, D.L.; A.I.M.E. Trans., 186, 66 (1949).

24. Kobayashi, R., Katz, D.L.; Ind. Eng. Chem., 45, 440 (1953).

25. Krichevsky, I.R., Kasarnovsky, J.S.; J. Am. Chem. Soc., 57, 2168 (1935).

26. Marshall, D.R.; Ph.D. Thesis, William Marsh Rice University, Houston, Texas (1962).

27. Marshall, D.R., Shozaburo, S., Kobayashi, R.; A.I.Ch.E. Journal, 10, 202 (1964).

28. McKetta, J.J., Katz, D.L.; Ind. Eng. Chem., 40, 853 (1948).

29. McKoy, V., Sinanoglu, O.; J. Chem. Phy., 38, 2946 (1963).

30. Miller, B., Strong, E.R.; Am. Gas Assoc. monthly, 28, 63 (1946).

31. Noaker, L.J., Katz, D.L.; A.I.M.E. Trans., 201, 237 (1954).

32. Otto, F.D.; M.Sc. Thesis, University of Alberta (1959).

33. Othmer, F.D., White, R.E.; Ind. Eng. Chem., 34, 952 (1942).

34. Parent, J.D.; "Storage of Natural Gas as Hydrates", Bulletin No. 1, I.G.T., Chicago, January (1948).

35. Powell, H.M.; J. Chem. Soc., 61 (1948).

36. Powell, H.M.; J. Chem. Soc., 2658 (1954).

37. Poettmann, F.H., Katz, D.L.; Ind. Eng. Chem., 37, 847 (1945).

38. Prausnitz, J.M., Myers, A.L.; A.I.Ch.E. Jour., 9, 1 (1963).

39. Reamer, H.H., Sage, B.H., Lacey, W.N.; Ind. Eng. Chem., 43, 2515 (1951).

40. Reamer, H.H., Selleck, F.T., Sage, B.H.; A.I.M.E. Trans., 195, 197 (1952).

41. Roberts, O.L., Brownscombe, E.R., Howe, L.S.; Oil and Gas Journal, 39 (30), 37 (1940).

42. Robinson, D.B.; "Application of Phase Rule to Study of Gas Hydrates", Unpublished Report (1947).

43. Scauzillo, F.R.; Chem. Eng. Prog., 52, 324 (1956).

44. Schaeffer, W.D.; "Advances in Petroleum Chemistry and Refining", Vol. 6, Interscience (1962).

45. Sherwood, T.K.; "A Course in Process Design", M.I.T. Press (1963).

46. Shozaburo, S., Marshall, D.R., Kobayashi, R.; A.I.Ch.E. Journal, 10, 734 (1964).

47. Shozaburo, S., Kobayashi, R.; A.I.Ch.E. Journal, 11, 96 (1965).

48. Sortland, L.D.; M.Sc. Thesis, University of Alberta (1962).

49. Snell, E.; M.Sc. Thesis, University of Alberta (1961).

50. Stackelberg, M. von, Muller, H.R.; J. Chem. Phy., 19, 1319 (1951).

51. Stackelberg, M. von, Muller, H.R.; Z. Electrochem, 58, 25, 40, 99 (1954).

52. Unruh, C.H., Katz, D.L.; A.I.M.E. Trans., 186, 83 (1949).

53. Villard, P.; Compt. Rend., 119, 368 (1894).

54. Waals, J.H. van der, Platteeuw, J.C.; Molecular Physics, 1, 91 (1958).

55. Waals, J.H. van der, Platteeuw, J.C.; Recueil, T. 78, No. 2, 126, February (1959).

56. Waals, J.H. van der, P atteeuw, J.C.; "Advances in Chemical Physics", Vol. 2, Interscience (1959).

57. Waals, J.H. van der and Platteeuw, J.C.; Private communication.

58. Wiebe, R., Gaddy, V.L.; J. Am. Chem. Soc., 61, 315 (1938).

59. Wiebe, R., Gaddy, V.L.; J. Am. Chem. Soc., 62, 815 (1940).

60. Wilcox, W.I., Carson, D.B., Katz, D.L.; Ind. Eng. Chem., 33, 662 (1941).